Part 2:

Lower Atmosphere

Wayan Suparta

Location of observation

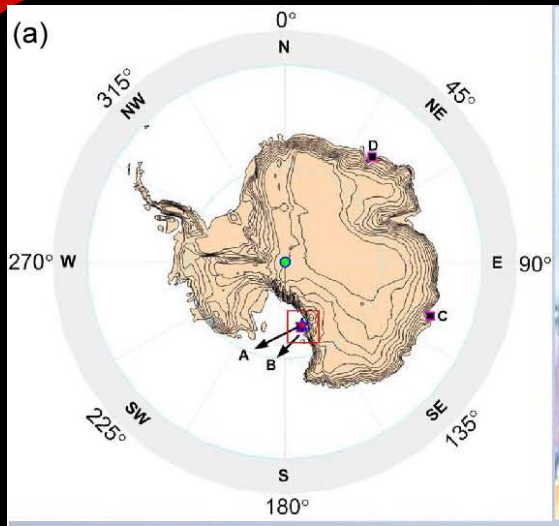

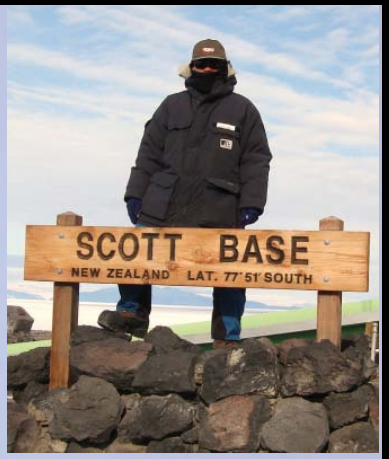

Scott Base, Antarctica


MCMURDO STATION
ANTARCTICA

Mt. Erebus


WAYAN SURATA

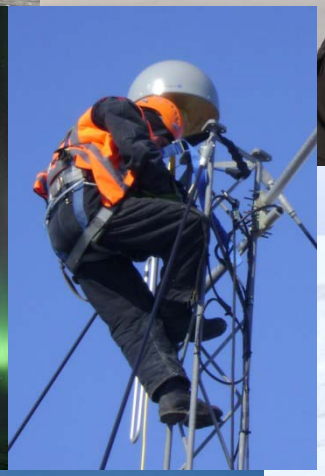


Trimble
5700


ZK-HNC


Trimble


P


WAYAN

Northern hemisphere: Iceland

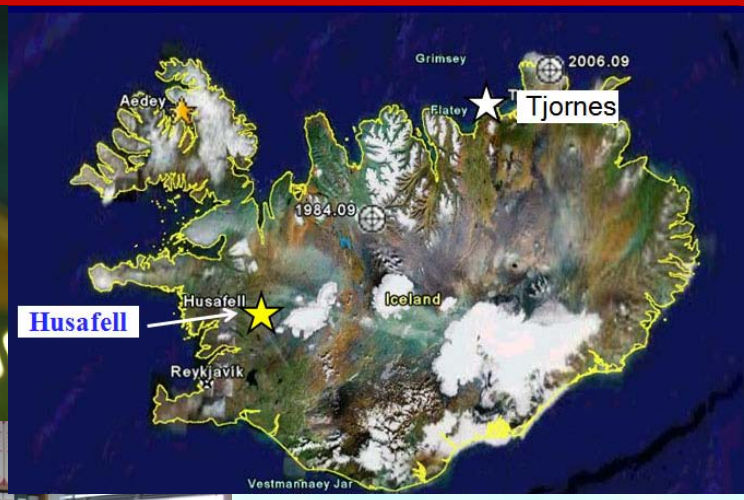

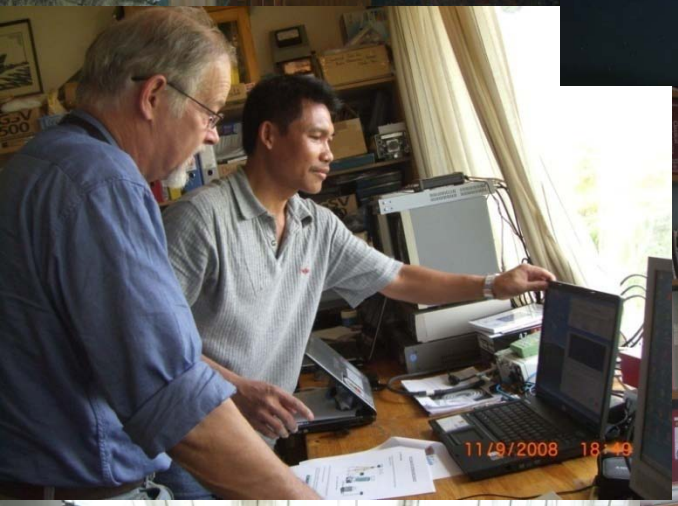

Computing the Tropospheric Delay and PWV Using GPS Measurements

- Zenith Total Delay (ZTD)
- Zenith Hydrostatic Delay (ZHD)
- Zenith Wet Delay (ZWD)
- Mapping function
- Elevation angle

The concept

The work based on GPS Meteorology concept

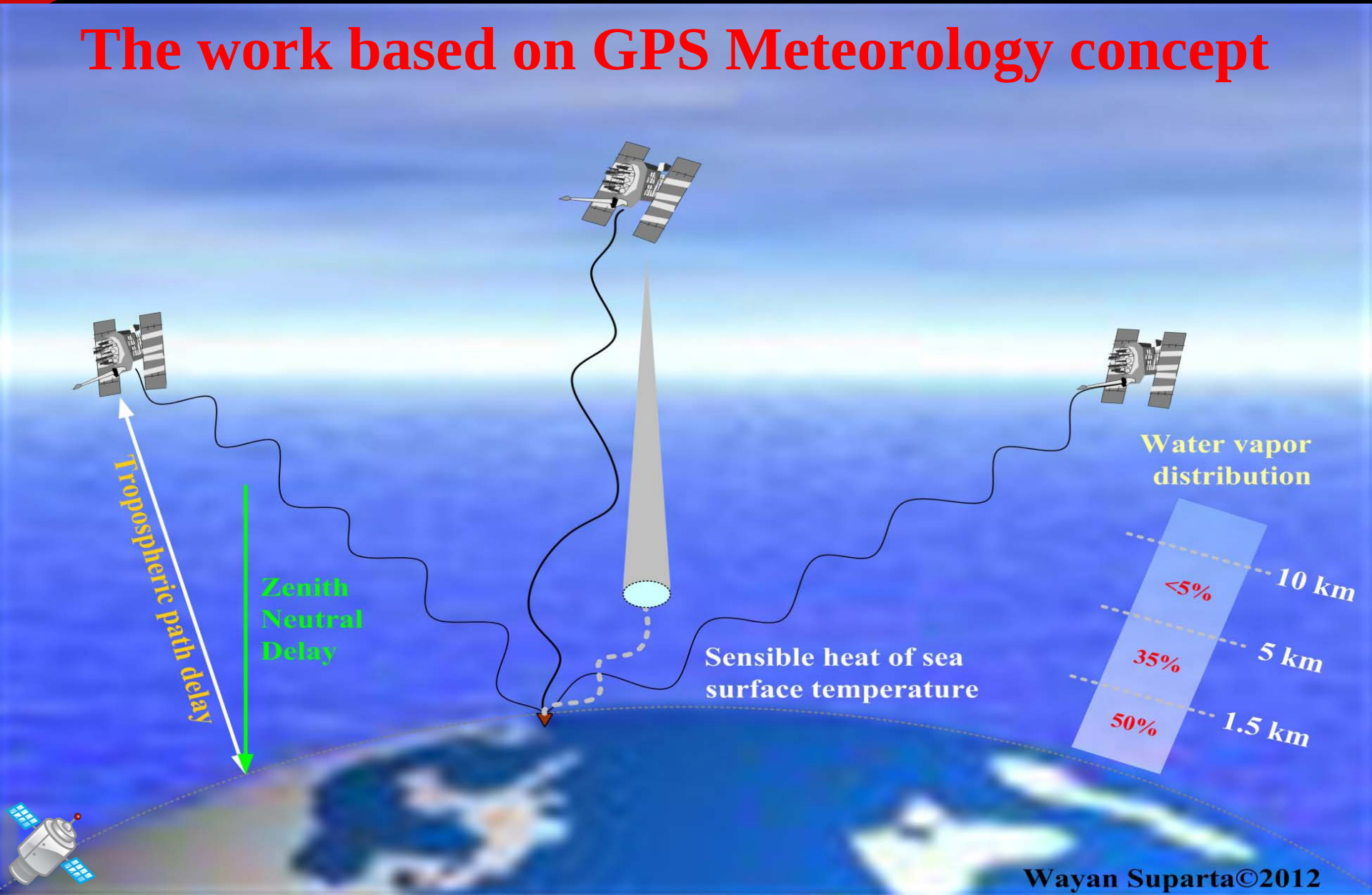

Tropospheric Path Delay

Signal from GPS

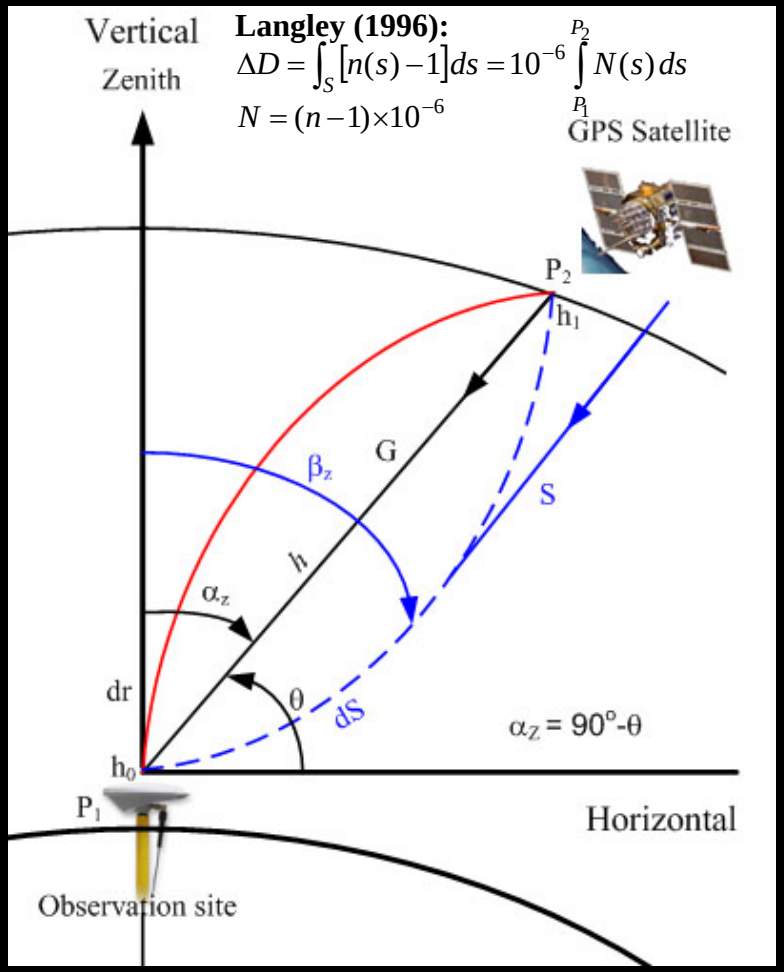

(a)

Modeling of tropospheric delay

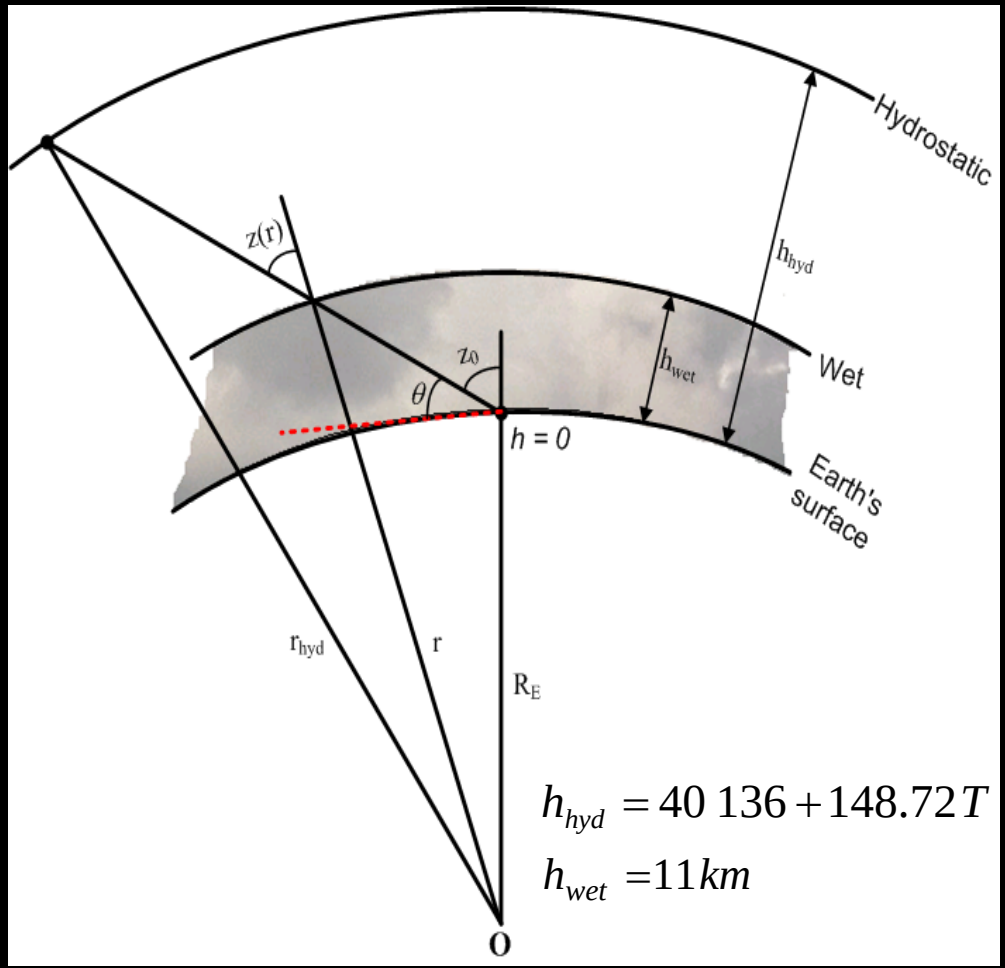

(b)

Geometry of the tropospheric path delay

In the equilibrium state, the total tropospheric delay in the zenith direction can be formulated as

$$\mathbf{ZTD = ZHD + ZWD} \qquad \mathbf{(1)}$$

To account the satellite elevation angle during the propagation, Davis et al. (1985) formulated the total tropospheric delay (ΔD) as,

$$\Delta D = m_h(\theta)\, SHD + m_w(\theta)\, SWD \qquad (2)$$

where *m* is mapping function, *SHD* and *SWD* are slant hydrostatic delay and slant wet delay.

From Fig. (b), the corresponding lengths are $r_{hyd} = R_E + h_{hyd}$ and $r = R_E + h_{wet}$

The empirical representation of refractivity, as a function of height *h* above the surface can be written as (Hofmann-Wellenhof et al., 2001),

$$N_j^{Trop}(r) = N_{j,0}^{Trop}\left(\frac{r_j - r}{r_j - R_E}\right)^4 \qquad (3)$$

Goad and Goadman (1974), Black (1978), Black and Eisner (194) has an effort to calculate the tropospheric delay with accounting the zenith elevation angle. Remondi (1984) reported the Hopfield model with a series expansion of the integrand. Finally, Modified Hopfield model, as a function of height *h* above the surface (see Fig. b) with accounted the satellite elevation angle is reported by Hofmann-Wellenhof et al. *(*2001), and corrected by Suparta et al. (2008), with ΔD or ZTD can be written as follows:

$$ZTD = 10^{-12} N_{j,0}^{Trop} \left[\begin{array}{l} 1 + 4a_j \frac{r_j^2}{2} + \left(6a_j^2 + 4b_j\right)\frac{r_j^3}{3} + 4a_j\left(a_j^2 + 3b_j\right)\frac{r_j^4}{4} + \left(a_j^4 + 12a_j^2 b_j + 6b_j^2\right)\frac{r_j^5}{5} + \ldots \\ 4a_j b_j\left(a_j^2 + 3b_j\right)\frac{r_j^6}{6} + b_j^2\left(6a_j^2 + 4b_j\right)\frac{r_j^7}{7} + 4a_j b_j^3 \frac{r_j^8}{8} + b_j^4 \frac{r_j^9}{9} \end{array} \right] \quad (4)$$

where

$$a_j = -\frac{\sin\theta}{h_j} \quad \text{and} \quad b_j = -\frac{\cos^2\theta}{2h_j R_E}$$

θ is satellite elevation angle (deg),
R_E is taken as 6378137 m
h is effective height and *j* ➔ wet and hydrostatic
$N_{j,0}^{Trop}$ is the total refractivity at the surface of the Earth

Computation of refractivity at the surface

$$N_{j,0}^{Trop} = N_{hyd,0}^{Trop} + N_{wet,0}^{Trop} = \underbrace{k_1 \frac{P}{T_K}}_{hydrostatic} + \underbrace{\left(\underbrace{k_2' \frac{P_{wet}}{T_K} Z_{wet}^{-1}}_{dipole\ \ moment} + \underbrace{k_3 \frac{P_{wet}}{T_K^2} Z_{wet}^{-1}}_{dipole\ \ orientation} \right)}_{wet} \quad (5)$$

where inverse compressibility factors (Z^{-1}) defined by Owen (1967):

$$Z_{dry}^{-1} = 1 + P_{dry} \left[57.97 x 10^{-8} \left(1 + \frac{0.52}{T_K} \right) - 9.4611 x 10^{-4} \frac{T}{T_K^2} \right] \quad (6)$$

$$Z_{wet}^{-1} = 1 + 1650 \frac{P_{wet}}{T_K^3} \left(1 - 0.01317 T + 1.75 x 10^{-4} T^2 + 1.44 x 10^{-6} T^3 \right) \quad (7)$$

$P_{dry} = P_{tot}$, the surface pressure measured by barometer (in mbar or hPa)
T and T_K are in C and Kelvin, respectively.

P_{wet} is obtained from relative humidity (H) as recommended by World Meteorological Organization Technical Note No. 8 (WMO 2000) :

$$P_{wet} = \frac{H}{100}\exp\left(-37.2465 + 0.213166T_K - 2.56908x10^{-4}T_K^2\right) \quad (8)$$

The refractivity constant (k) for **(5)** is listed in Table 1.

Table 1. Determinations of the refractivity constants

Reference	k_1 (K mbar^{-1})	k_2 (K mbar^{-1})	k_3 (K^2 mbar^{-1}) x 10^5
Smith & Weintraub (1953)	77.61 ± 0.01	72 ± 9	3.75 ± 0.03
Boudouris (1963)	77.59 ± 0.08	72 ± 11	3.75 ± 0.03
Thayer (1974)	77.61 ± 0.01	47.79 ± 0.08	3.776 ± 0.04
Hill et al. (1982)	-	98 ± 1	3.583 ± 0.03
Hill (1988)	-	102 ± 1	3.578 ± 0.03
Clynch (1990)	77.604 ± 0.02	75 ± 0.1	3.75 ± 0.01
Bevis et al. (1992)	77.60 ± 0.05	70.4 ± 2.2	3.739 ± 0.012
Bevis et al. (1994)	77.60 ± 0.09	69.4 ± 2.2	3.701 ± 1200

$$k_2' = k_2 - k_1\frac{M_w}{M_d} = (22.1 \pm 2.2)$$

M_w is the molar mass of water vapor (28.9644 kg kmol^{-1}) and M_d is the molar mass of dry air (18.0152 kg kmol^{-1})

Mapping Function

A mapping function is developed due to the tropospheric delay is the shortest in the zenith direction and becomes larger with increasing zenith angle. Instead, the individual delays are mapped from each individual satellite direction to a single zenith delay. Mapping functions account for the delay seen by each satellite and map them to the zenith direction.

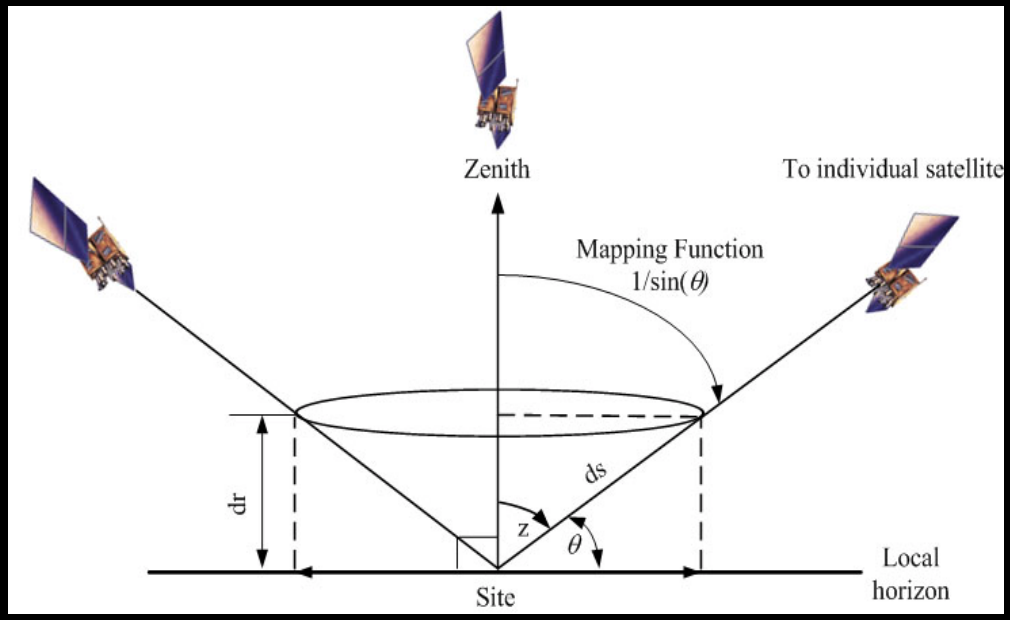

Cosecant mapping function:

$$m(z) = \frac{1}{\cos z} \equiv \sec z \quad \Rightarrow \quad m(\theta) = \frac{1}{\sin \theta}$$

(9)

Because of the curvature of the atmosphere, this zenith angle changes along the ray. Due to the large deviations for lower elevation angles, this function is limited for use above about 60 degrees elevation.

Niell Mapping function

- There are type of mapping functions includes Chao (1972), Davis et al. (1985), Marini (1972), Niell (1996), and Boehm (2006).
- Niell has developed hydrostatic and wet mapping functions with new forms and their combined, use to reduces errors in geodetic estimation for observations as low as 3° in elevation.
- The hydrostatic mapping function, which has normalized to yield a value of unity at the zenith, can be written as

$$m_h(\theta) = m(\theta) + \Delta m(\theta)$$
$$= \frac{1+\left(a/(1+b/(1+c))\right)}{\sin\theta+(a/\sin\theta+(b/\sin\theta+c))} + \left[\frac{1}{\sin\theta} - f\left(\theta, a_{ht}, b_{ht}, c_{ht}\right)\right]h \qquad (10)$$

- The coefficients *a*, *b* and *c* are interpolated from the latitude of the GPS site and take seasonal variations into account.
- Here, $f(\theta, a_{ht}, b_{ht}, c_{ht})$ represents the three-term continued fraction in the Marini mapping function,

$$f\left(\theta, a_{ht}, b_{ht}, c_{ht}\right) = \frac{1+\left(a_{ht}/(1+b_{ht}/(1+c_{ht}))\right)}{\sin\theta+\left(\sin\theta+a_{ht}/(\sin\theta+b_{ht}/(\sin\theta+b_{ht}))\right)} \qquad (11)$$

where the coefficients $a_{ht} = 2.53 \times 10^{-5}$, $b_{ht} = 5.49 \times 10^{-3}$ and $c_{ht} = 1.14 \times 10^{-3}$ were determined by a least-squares fit to the height corrections at the nine elevation angles.

- For the hydrostatic component, these coefficients are determined based on height, latitude and DoY (day of year), which can be extracted from Table 2.

Table 2. Coefficients of the hydrostatic mapping function

Coefficient	φ = 15°	φ = 30°	φ = 45°	φ = 60°	φ = 75°
a_{avg}	$1.2769934.10^{-3}$	$1.2683230.10^{-3}$	$1.2465397.10^{-3}$	$1.2196049.10^{-3}$	$1.2045996.10^{-3}$
b_{avg}	$2.9153695.10^{-3}$	$2.9152299.10^{-3}$	$2.9288445.10^{-3}$	$2.9022565.10^{-3}$	$2.9024912.10^{-3}$
c_{avg}	$62.610505.10^{-3}$	$62.837393.10^{-3}$	$63.721774.10^{-3}$	$63.824265.10^{-3}$	$64.258455.10^{-3}$
a_{amp}	0.0	$1.2709626.10^{-5}$	$2.6523662.10^{-5}$	$3.4000452.10^{-5}$	$4.1202191.10^{-5}$
b_{amp}	0.0	$2.1414979.10^{-5}$	$3.0160779.10^{-5}$	$7.2562722.10^{-5}$	$11.723375.10^{-5}$
c_{amp}	0.0	$9.0128400.10^{-5}$	$4.3497037.10^{-5}$	$84.795348.10^{-5}$	$170.37206.10^{-5}$

- For the latitude range $15° \le |\varphi| \le 75°$,

$$F(\varphi,t) = F_{avg}(\varphi_i) + \left[F_{avg}(\varphi_{i+1}) - F_{avg}(\varphi_i)\right].\frac{\varphi-\varphi_i}{\varphi_{i+1}-\varphi_i} + \ldots$$
$$\left\{F_{amp}(\varphi_i) + \left[F_{amp}(\varphi_{i+1}) - F_{amp}(\varphi_i)\right].\frac{\varphi-\varphi_i}{\varphi_{i+1}-\varphi_i}\right\}.\cos\left(2\pi\frac{DoY-T_0}{365.25}\right) \qquad (12)$$

➢ For the latitude $|\varphi| \leq 15°$,

$$F(\varphi,t) = F_{avg}(15°) + F_{amp}(15°) \,.\, \cos\left(2\pi \frac{DoY - T_0}{365.25}\right) \qquad (13)$$

➢ For the latitude $|\varphi| \geq 75°$,

$$F(\varphi,t) = F_{avg}(75°) + F_{amp}(75°) \,.\, \cos\left(2\pi \frac{DoY - T_0}{365.25}\right) \qquad (14)$$

- The coefficients *a*, *b* and *c* in (10) were derived from temperature and relative humidity profiles of the U.S. Standard Atmosphere which is dependent on the latitude at North regions 15° (tropical), 30° (subtropical), 45° (mid-latitude), 60 and 75° (subarctic) for the months of January (Winter) and July (Summer) and takes seasonal variations into account.
- Niell assumes that the Southern and Northern hemispheres are anti-symmetric in time, *i.e.*, that the seasonal behavior is the same. In addition, he assumes the equatorial region is described by the 15° N latitude profile while the polar region are described by the 75° N latitude profile.
- T_0 is the day of year for "maximum winter" which set to 28 for northern hemisphere and 211 for the southern hemisphere.

- For Niell wet mapping function can be written as:

$$m_w(\theta) = \frac{1+\left(a_w/(1+b_w/(1+c_w))\right)}{\sin\theta+(a_w/\sin\theta+(b_w/\sin\theta+c_w))} \qquad (15)$$

- Interpolation of Niell wet mapping function can be extracted from Table 3:

Table 3. Coefficients of the wet mapping function

Coefficient	φ = 15°	φ = 30°	φ = 45°	φ = 60°	φ = 75°
a_{avg}	$5.8021879.10^{-4}$	$5.6794847.10^{-4}$	$5.8118019.10^{-4}$	$5.9727542.10^{-4}$	$6.1641693.10^{-4}$
b_{avg}	$1.4275268.10^{-3}$	$1.5138625.10^{-3}$	$1.4572752.10^{-3}$	$1.5007428.10^{-3}$	$1.7599082.10^{-3}$
c_{avg}	$4.3472961.10^{-2}$	$4.6729510.10^{-2}$	$4.3908931.10^{-2}$	$4.4626982.10^{-2}$	$5.4736039.10^{-2}$

  - For the latitude range $15° \le |\varphi| \le 75°$,

$$F(\varphi,t) = F_{avg}(\varphi_i) + \left[F_{avg}(\varphi_{i+1}) - F_{avg}(\varphi_i)\right].\frac{\varphi-\varphi_i}{\varphi_{i+1}-\varphi_i} \qquad (16)$$

  - For the latitude $|\varphi| \le 15°$,

$$F(\varphi,t) = F_{avg}(15°) \qquad (17)$$

  - For the latitude $|\varphi| \ge 75°$,

$$F(\varphi,t) = F_{avg}(75°) \qquad (18)$$

Boehm or Vienna Mapping Function

- Boehm et al. (2006) updated the "b" and "c" coefficients of the Marini continued fraction form, as shown in (5). However, the hydrostatic "a" coefficients are still valid for zero heights.
- This mapping function is called the hydrostatic Vienna Mapping Function (VMF1) when using the European Centre for Medium-Range Weather Forecasts (ECMWF) instead of the Numerical Weather Models (NWMs).
- The coefficient *c* shown in (10) is now modeled to remove the systematic errors as

$$c = c_0 + \left[\left(\cos\left(\frac{DoY - 28}{365}2\pi + \psi\right) + 1\right)\frac{c_{11}}{2} + c_{10}\right](1 - \cos\varphi) \qquad (19)$$

- Parameters c_0, c_{10}, c_{11} and Ψ needed for computing coefficient c is

hemisphere	c_0	c_{10}	c_{11}	ψ
northern	0.062	0.001	0.005	0
southern	0.062	0.002	0.007	π

- With VMF, errors in the hydrostatic zenith delays interpolated from NWMs will be 1/3 or approximately 4 mm in the station height, or 20 mm for wrong used mapping function.

Example Mapping Function Results

Presented at ICICI-BME 2011

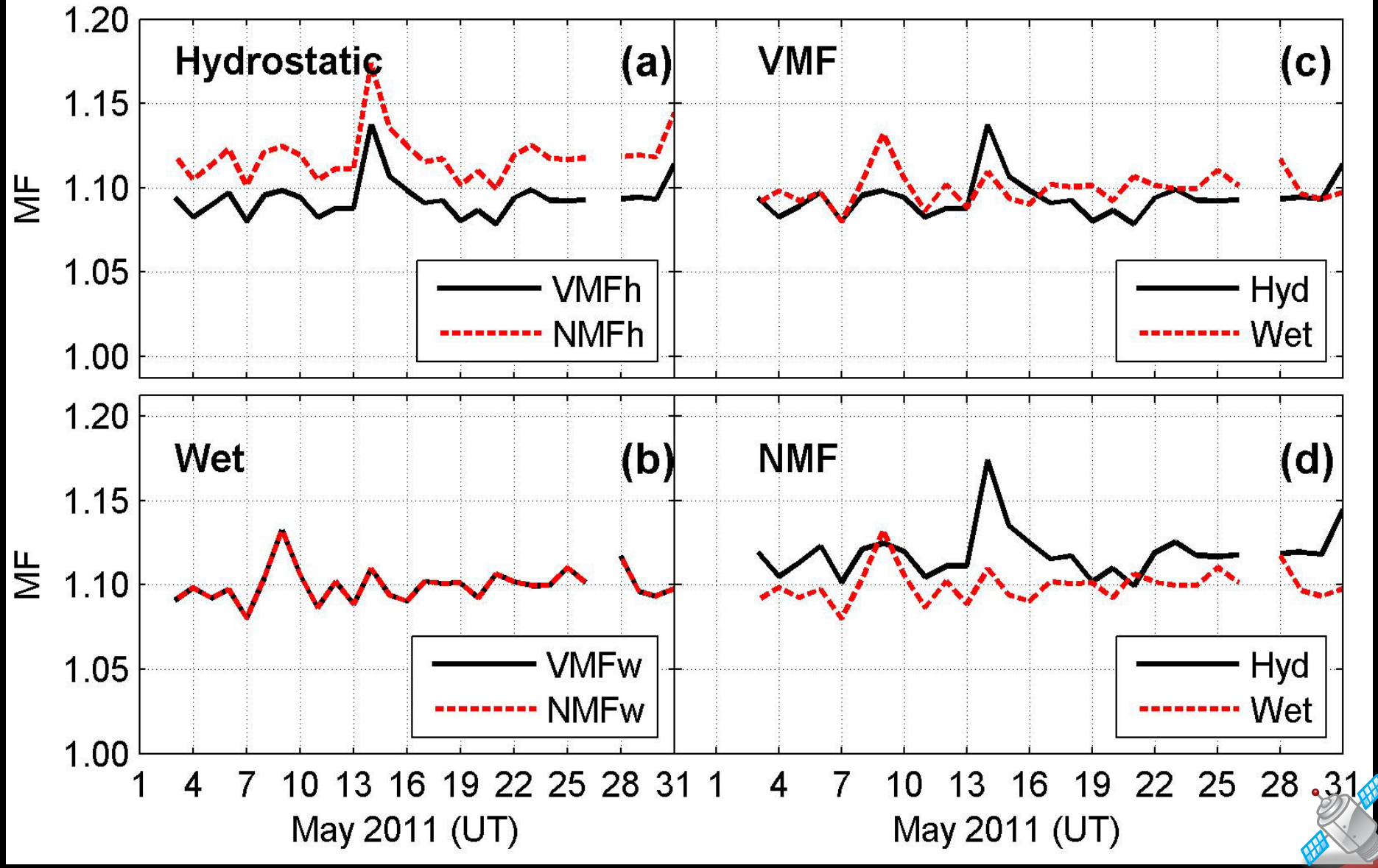

ZHD and ZWD

- There are a few models developed for ZHD, for example: Hopfield (1969), Saastamoinen (1973), Davis (1985), Baby et al. (1988), and Modified Hopfield (1974).
- The Saastamoinen model has become popular among GPS users due to its accuracy. It uses the surface pressure measurements and a correction factor $f(\varphi,h)$ to correct the local gravitational acceleration at the center of mass of the atmospheric column.
- The expression for ZHD can be written as follows:

$$ZHD_{SAAS}(P,\varphi,h) = (2.2768 \pm 0.0024)\frac{P}{f(\varphi,h)} \qquad (20)$$

where

$$f(\varphi,h) = 1 - 0.00266\cos(2\varphi) - 0.00028h \qquad (21)$$

h is the height of the site above the ellipsoid (in km), φ is geographic latitude (deg), P is surface pressure in mbar (hPa), and $f(\varphi,h)$ is the correction factor for the local gravitational acceleration.

- To calculate the ZWD, it can be estimated from the numerical weather model defined as:

$$ZWD = 10^{-6} \int_{h_0}^{\infty} N_w(h)\, dh$$

(22), N_w is wet refractivity

- From (5), (7) and (8), the integral for ZWD computation can be written as :

$$ZWD = 10^{-6} \left(k_2' + \frac{k_3}{T_m} \right) R_v \int_{h_0}^{\infty} \rho_w Z_w^{-1} dh$$

→ IWV ($kg.m^{-2}$)

- The ZWD, however, cannot be sufficiently modeled by using surface meteorological data due to the irregular distribution of water vapor in the atmosphere. The GPS calculated ZWD (in meters) is obtained by

$$ZWD_{GPS} = ZTD_{GPS} - ZHD_{SAAS}$$

(23)

PWV computation

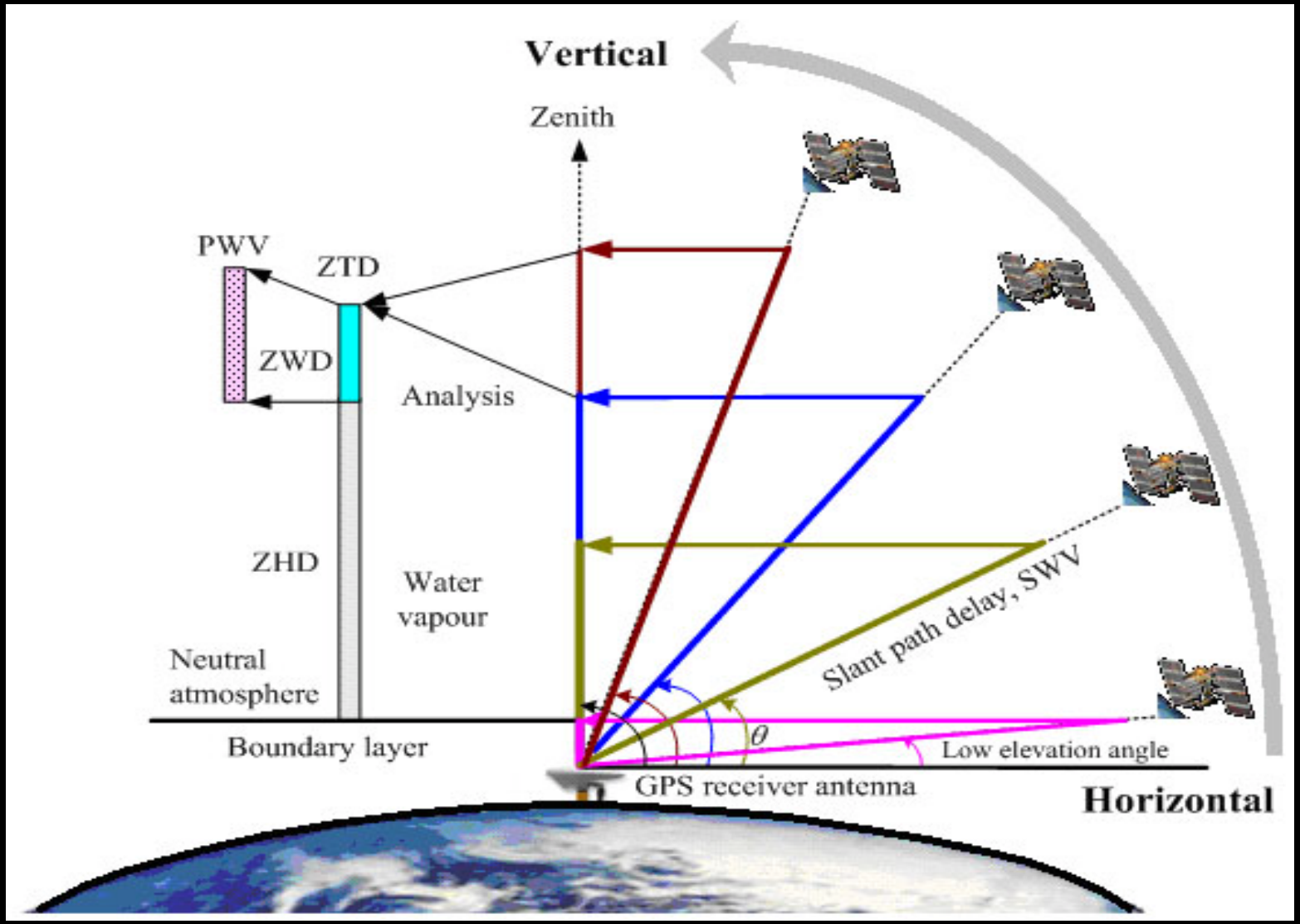

Figure D. The concept measurement of GPS PWV adapted from Nakamura (2003)

- IWV can be correlated with PWV as follows:

$$PWV = \frac{IWV}{\rho_{lw}}$$ (24), ρ_{lw} is the density of the liquid water (kg m^{-3})

- Bevis et al. (1992, 1994) proposed the equation compute PWV:

$$PWV = \pi(T_m) ZWD_{GPS}$$ with $$\pi(T_m) = \left[\rho_{lw} R_v \left(\frac{k_3}{T_m} + k_2' \right) \right]^{-1} 10^6$$ (25)

- T_m is the weighted mean temperature of the atmosphere (represented by N levels) is defined and approximated by Davis et al. (1985) as

$$T_m = \frac{\int (P_w / T_K) dz}{\int (P_w / T_K^2) dz} \approx \frac{\sum_{i=1}^{N} \frac{P_{wi}}{T_i} \Delta z_i}{\sum_{i=1}^{N} \frac{P_{wi}}{T_i^2} \Delta z_i}$$ (26)

Bevis et al. (1992, 1996)

$$T_m = 70.2 + 0.72\, T_K$$ (27)

Summary: PWV estimation

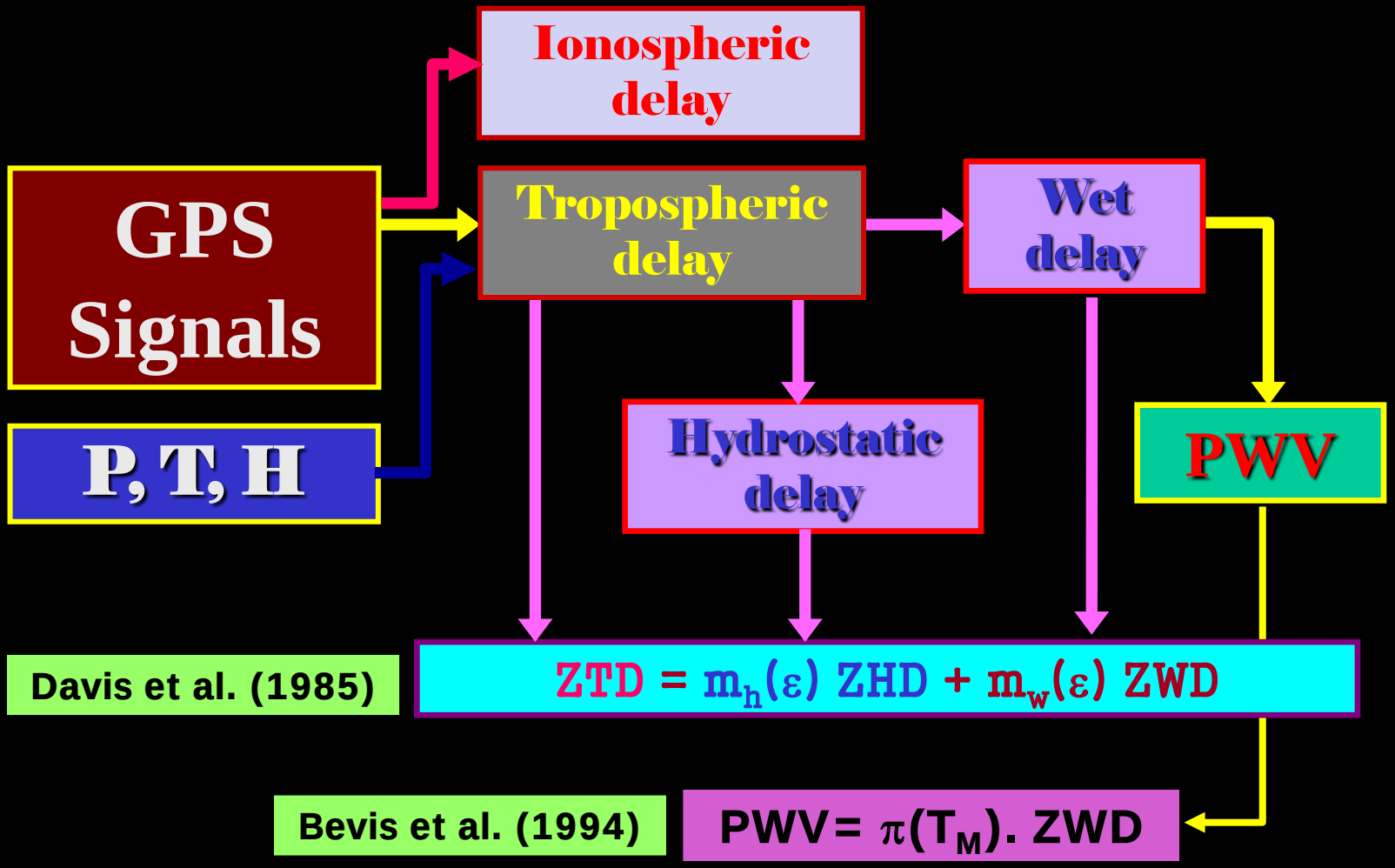

Source: Suparta et al. (2008): *JASTP* Vol. 70, 1419 - 1447

Example Results

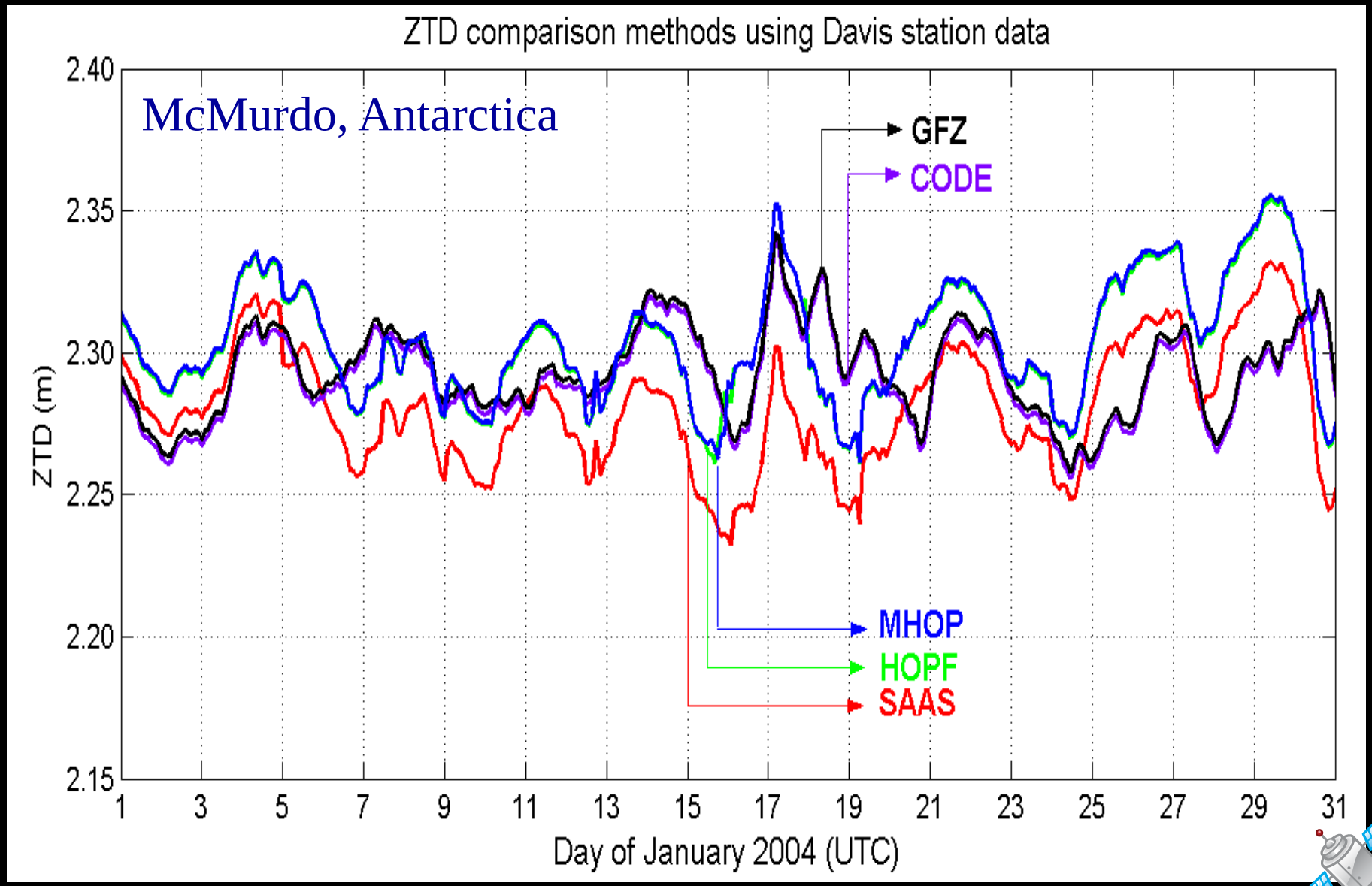

ZHD and the surface pressure

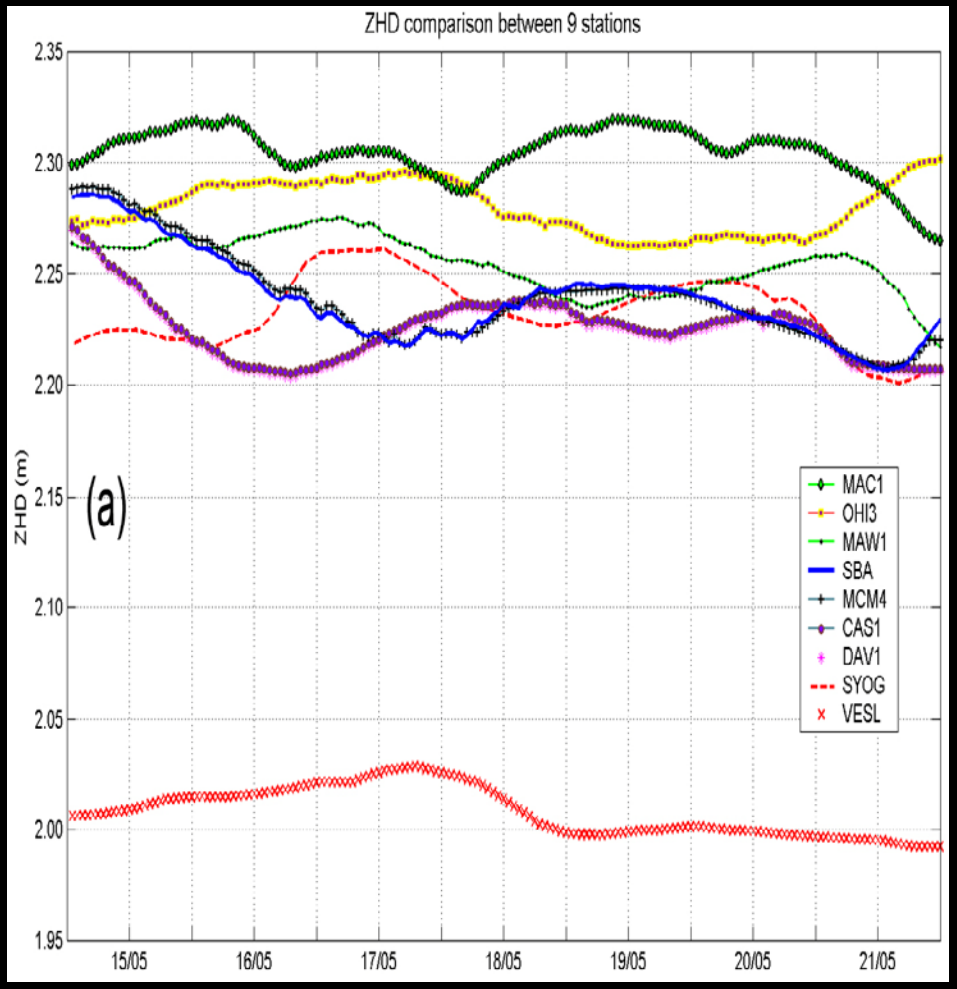

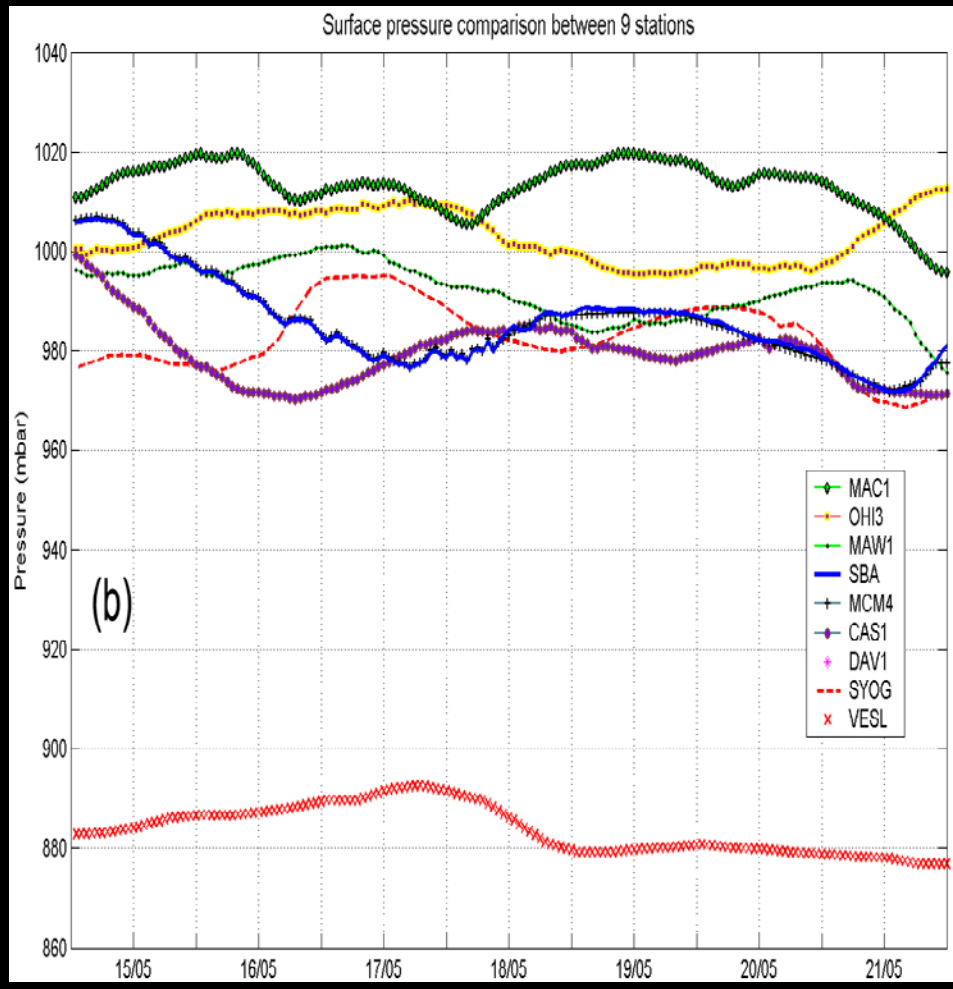

- ZHD is clearly very close to that of the surface pressure !

GPS PWV and the surface temperature

Presented at GUT2012

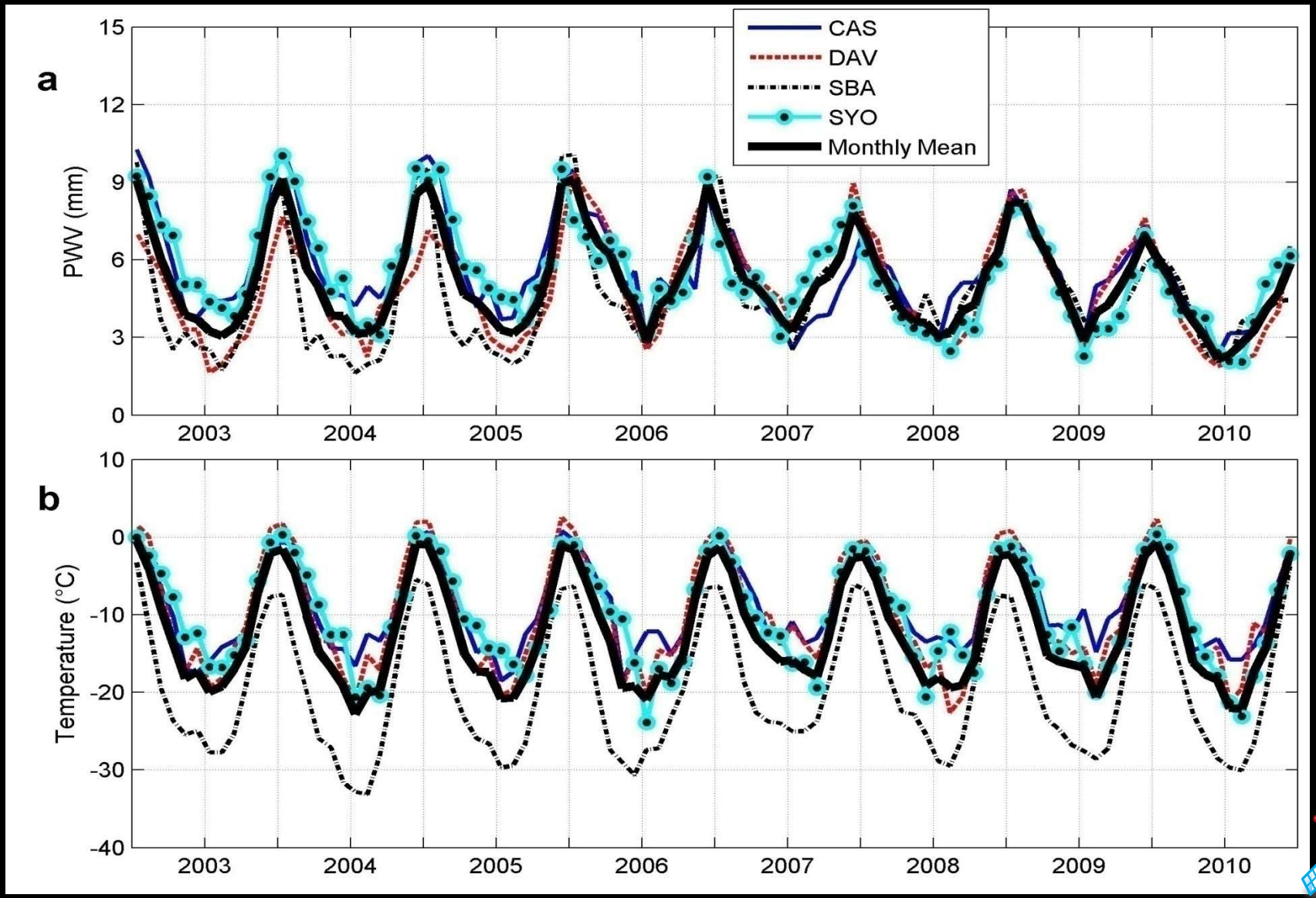

Annual cycle of GPS PWV

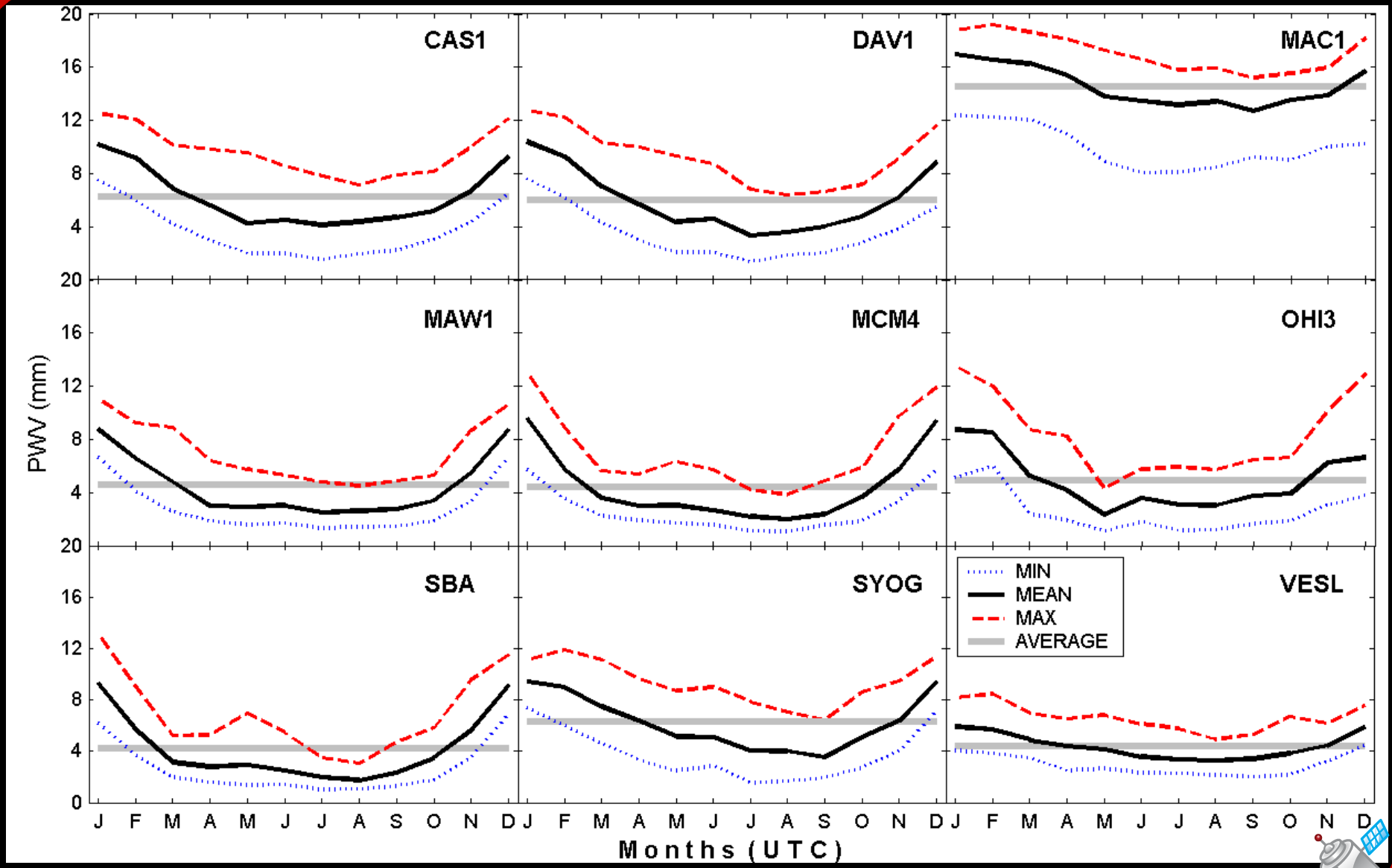

Average of 8 years (2003 – 2010)

GPS PWV vs surface temperature

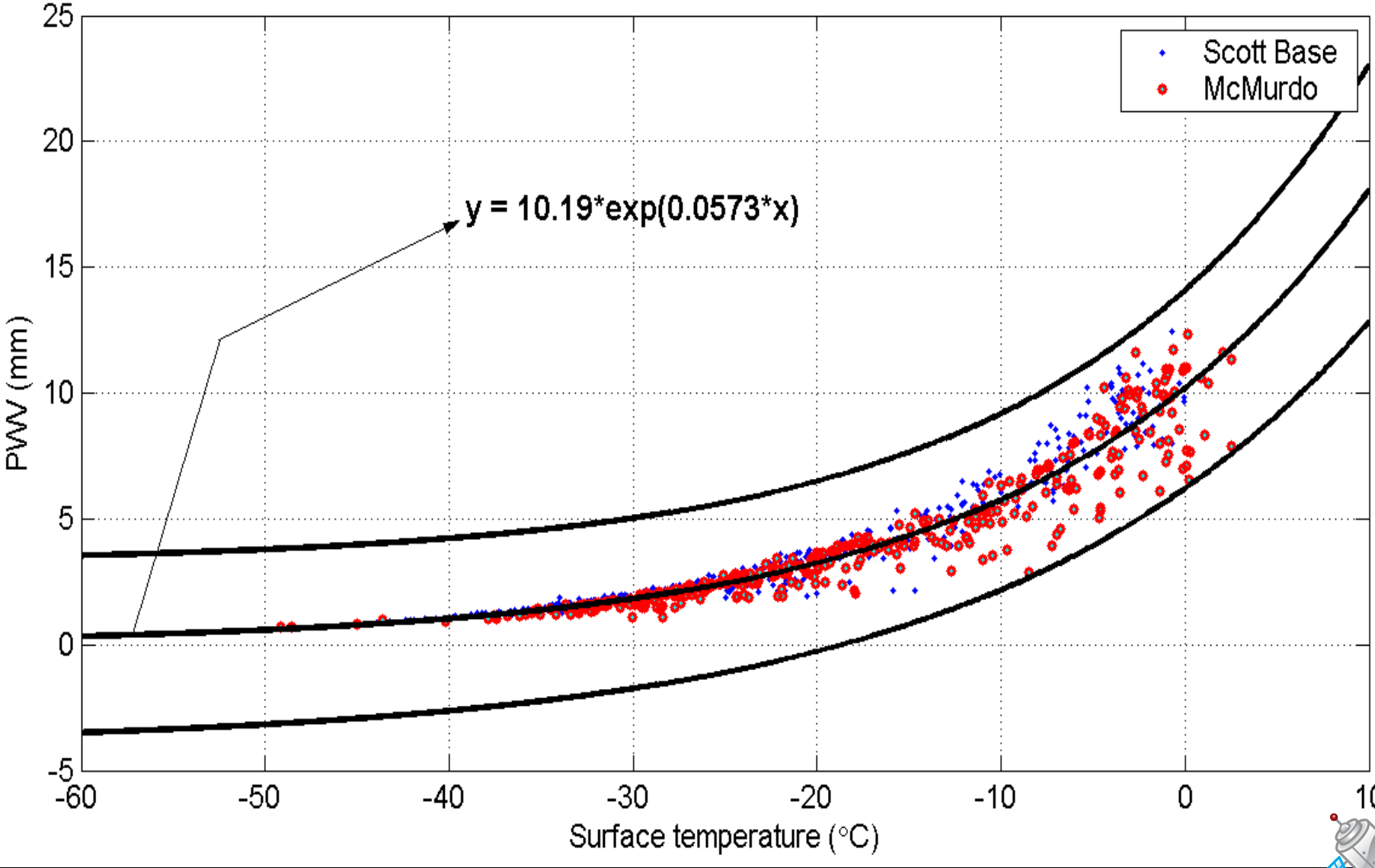

PWV from Radiosonde

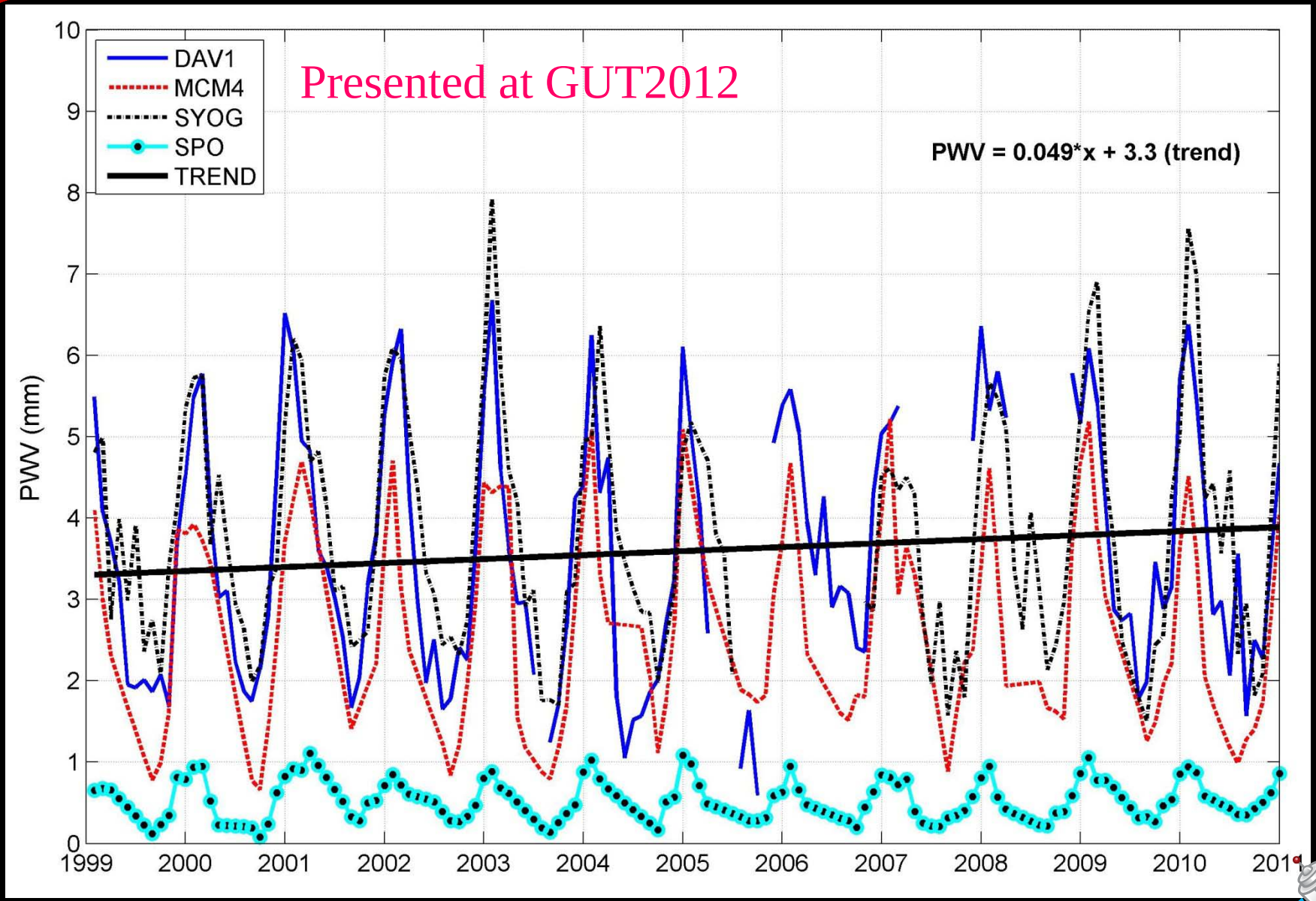

Real Time PWV Result

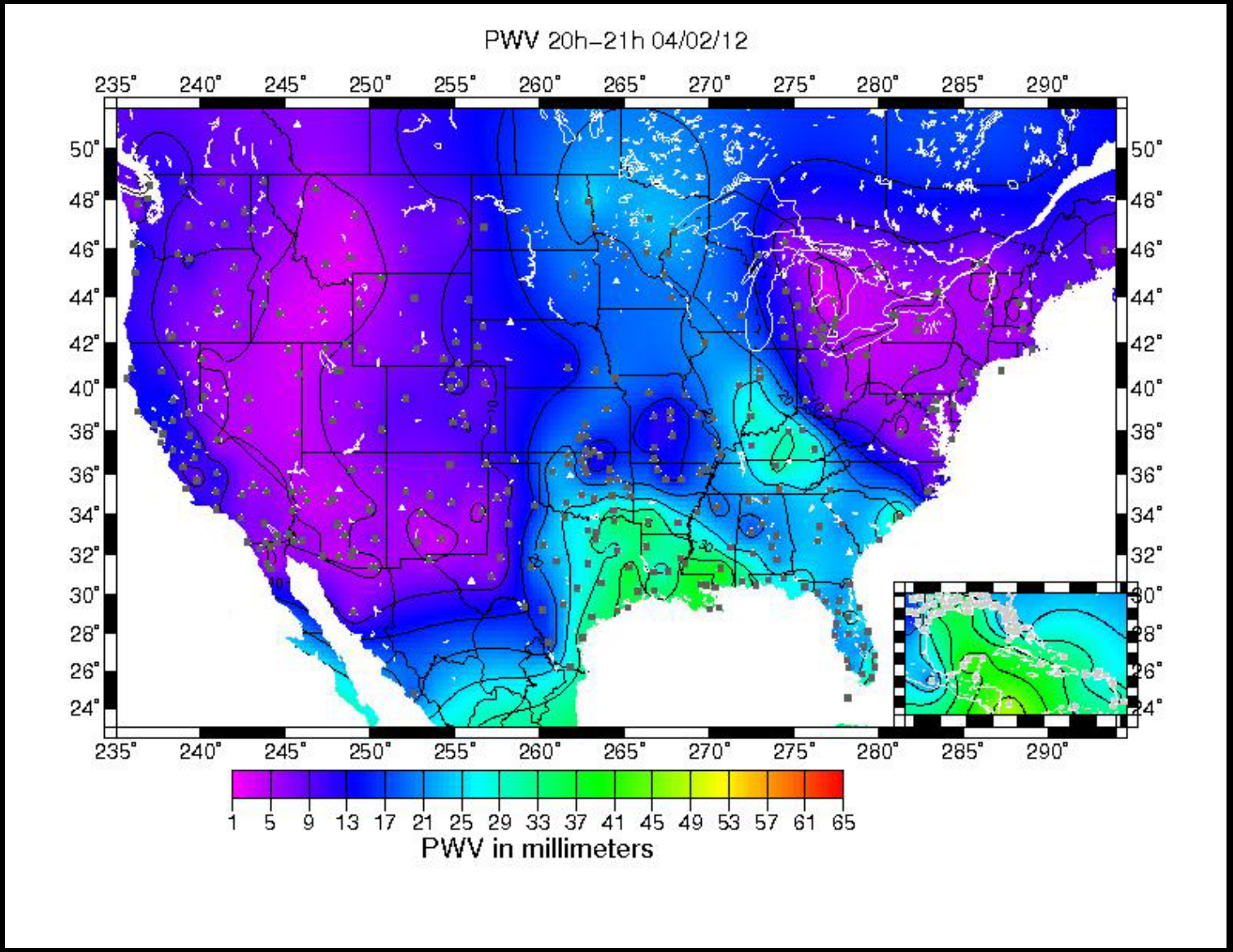

http://www.suominet.ucar.edu/map_images/

Real Time PWV Results

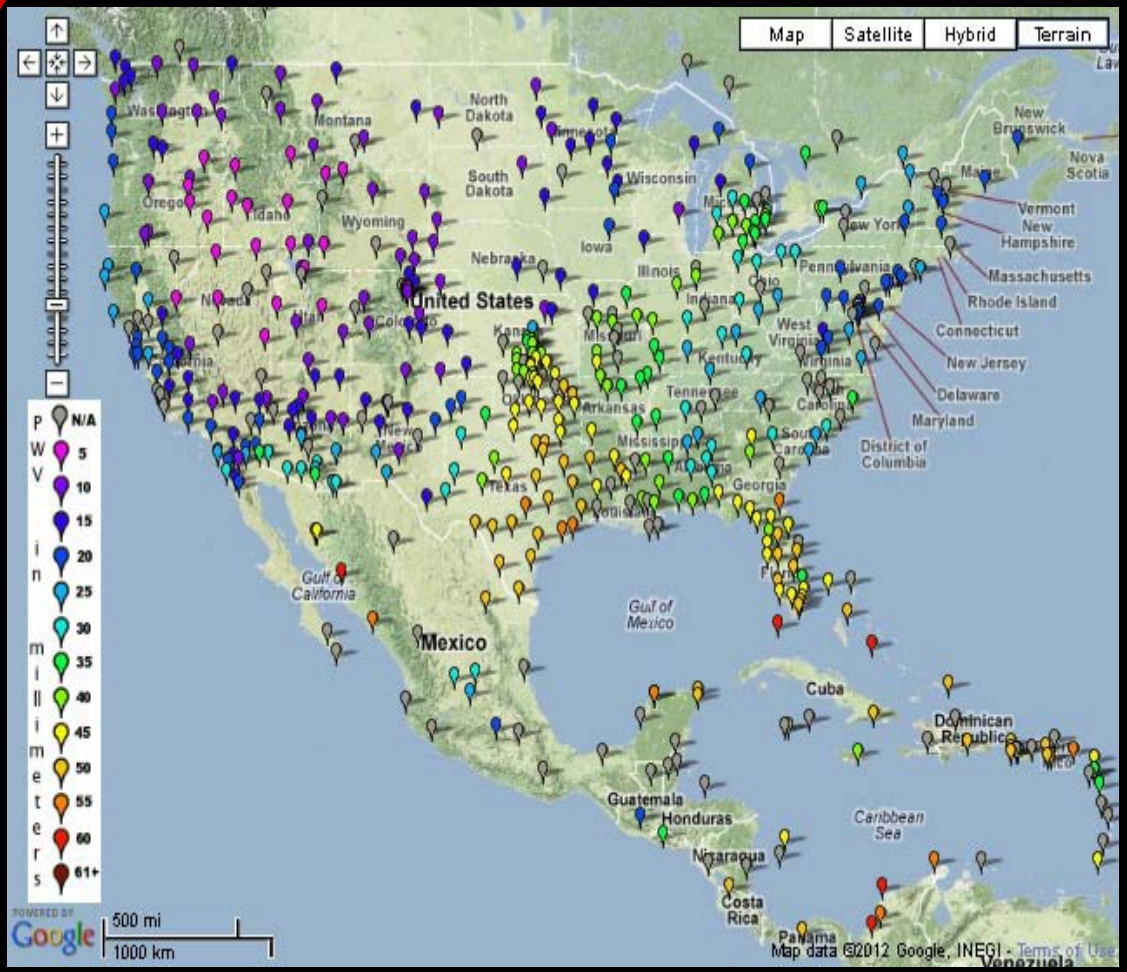

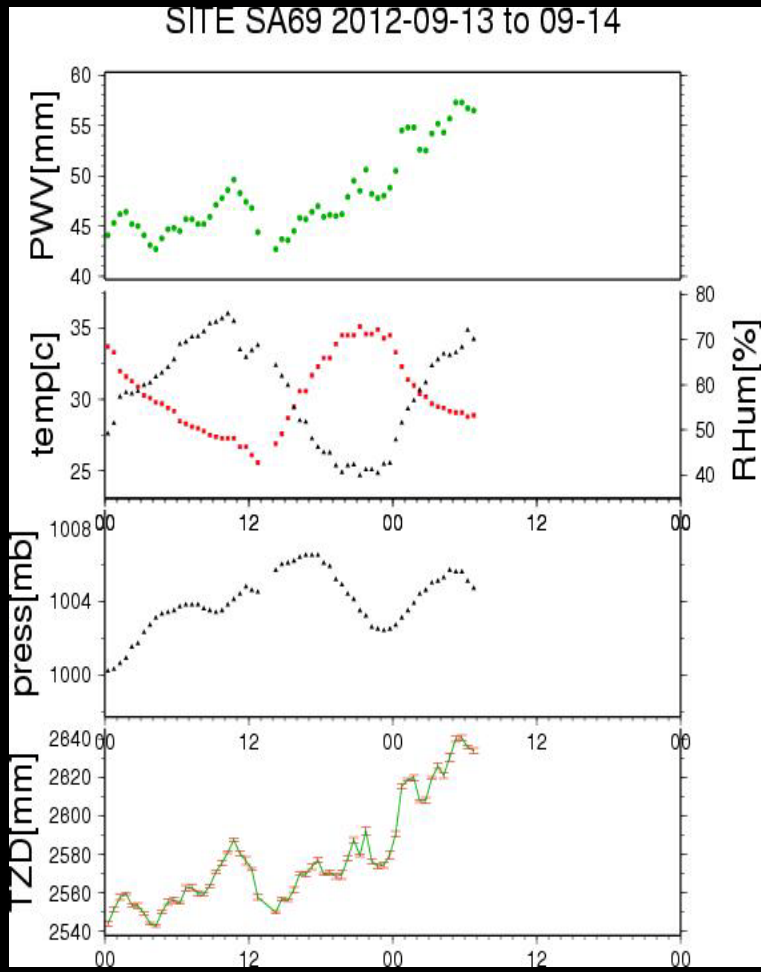

http://www.suominet.ucar.edu/index.html

GPS Meteorology products

Applications:

- Atmospheric monitoring
- Weather forecasting and prediction
- Global change and climate studies
- Severe weather alerts and advisories
- Natural climate variability detection: ENSO
- Space weather prediction (e.g. *FORMOSAT-3/COSMIC)*
- Sun-Earth Coupling → GCM
- Etc.

EX1: ENSO Monitoring

UMSK: 6.03°N latitude, 116.12°E longitude and height of 63.49 m

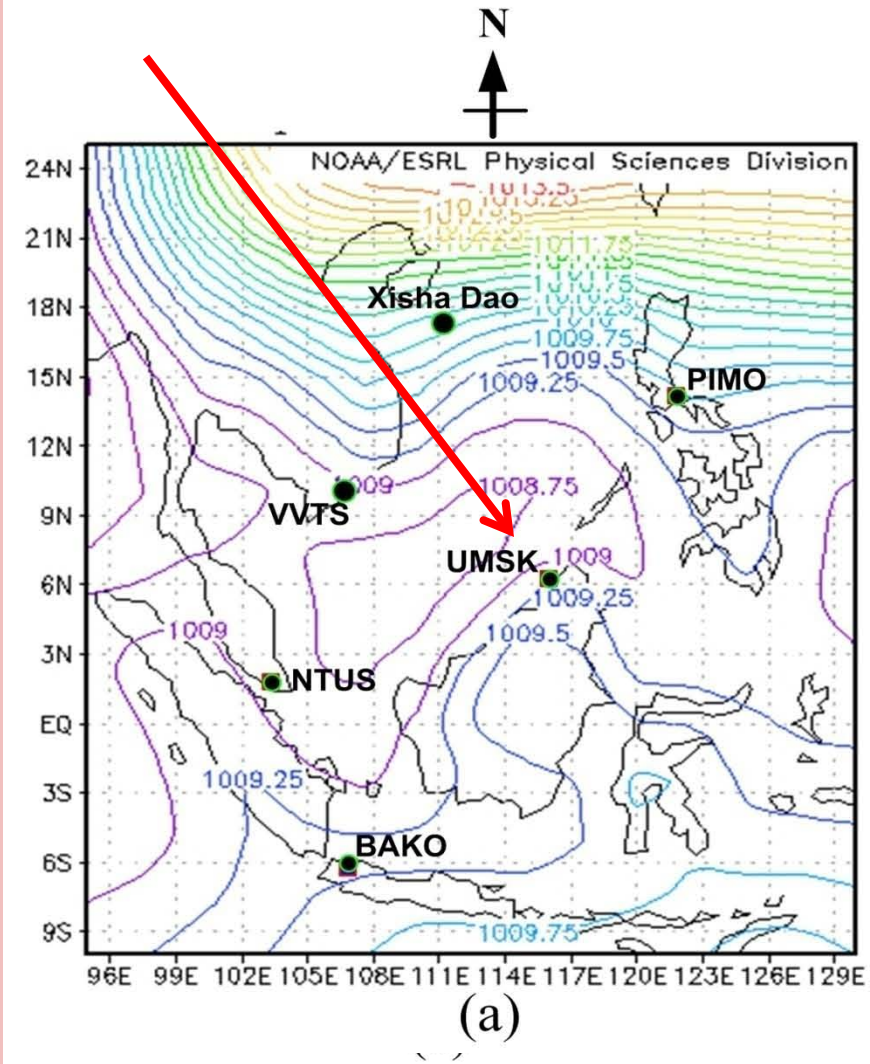

(a)

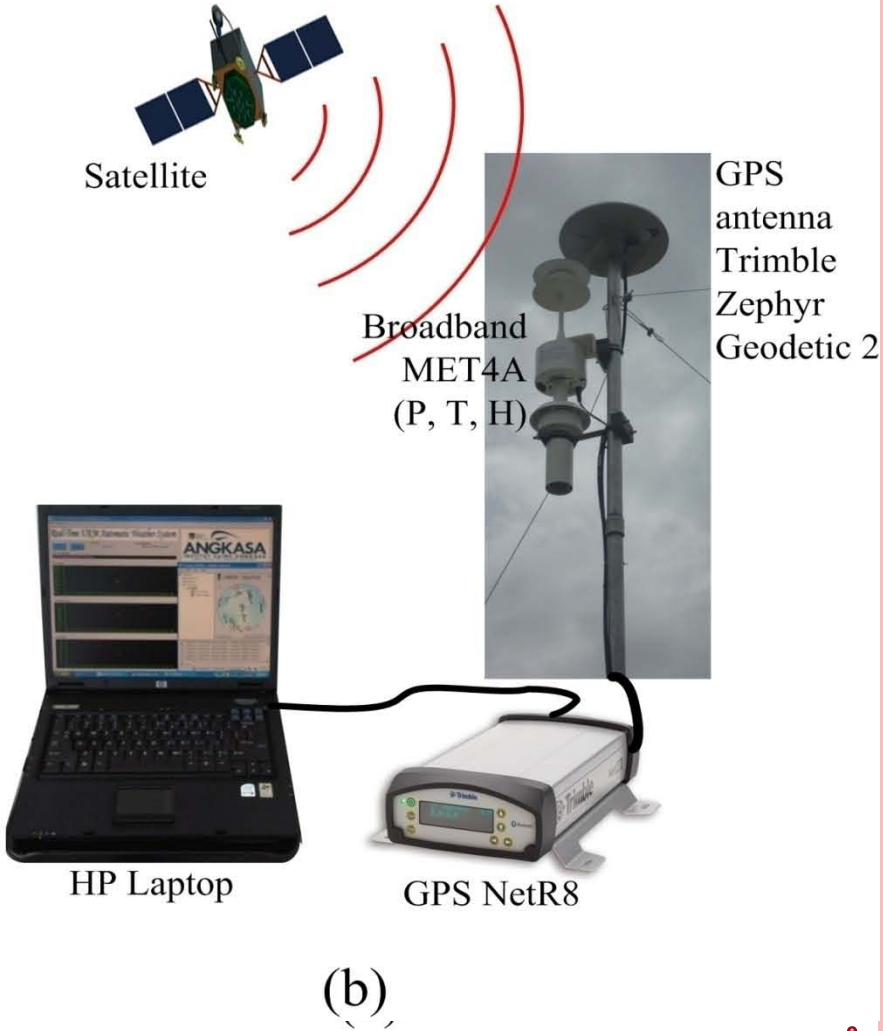

(b)

Location of observation

ENSO Episode

Cases of ENSO occurrence for the year of 2011 from SSTa data

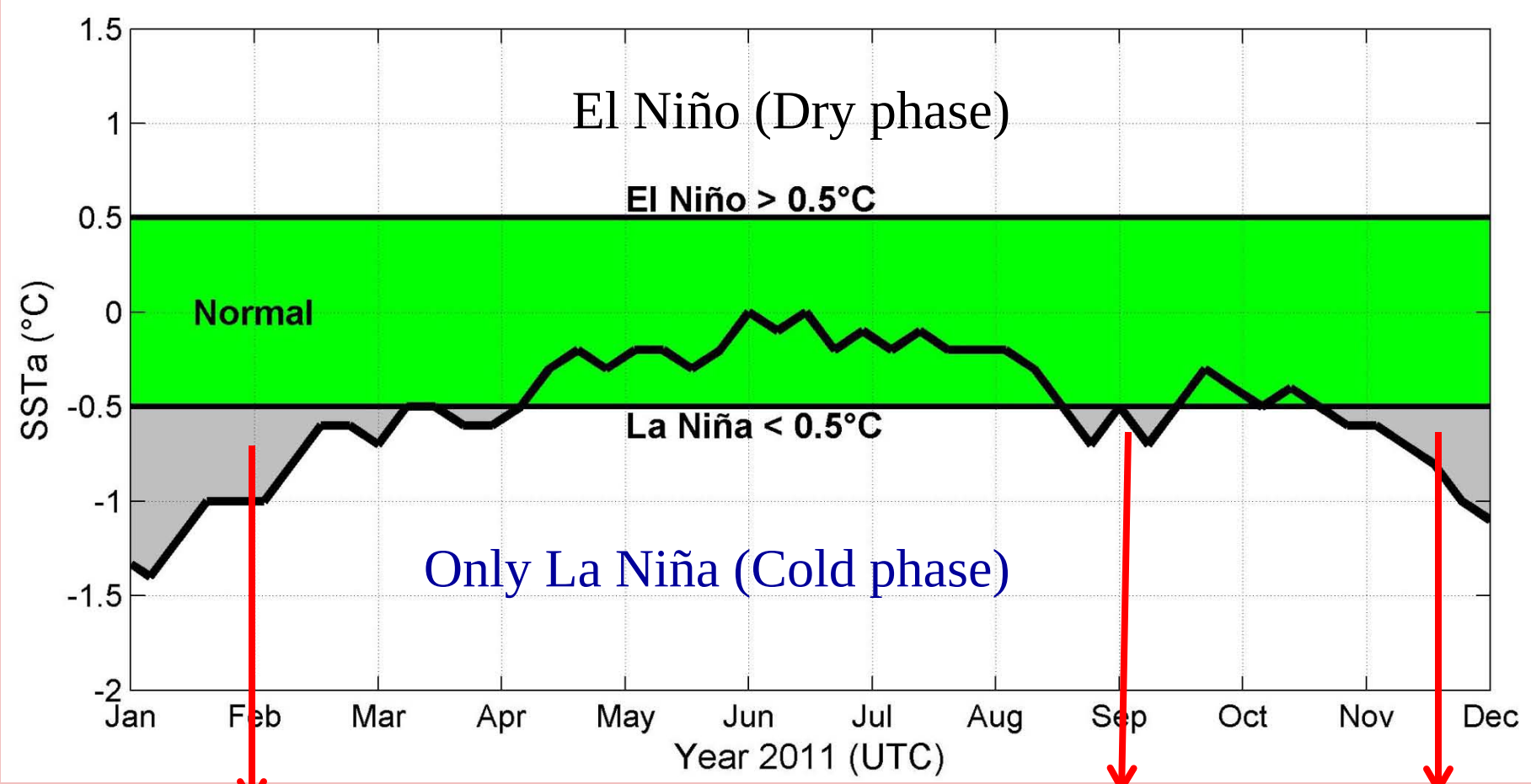

PWV on weekly basis

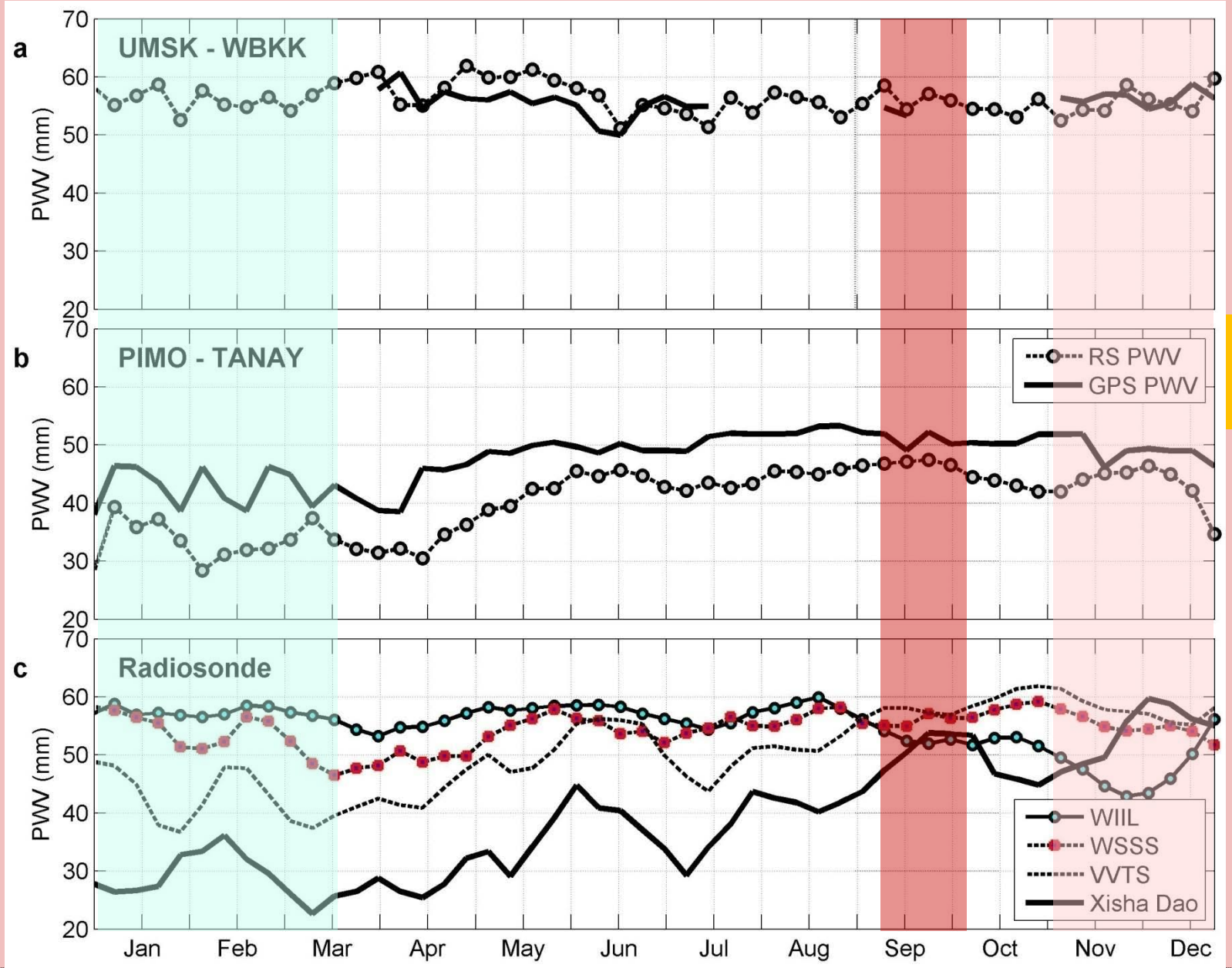

2011

Weekly basis

PWV at SSTa <-0.5 °C

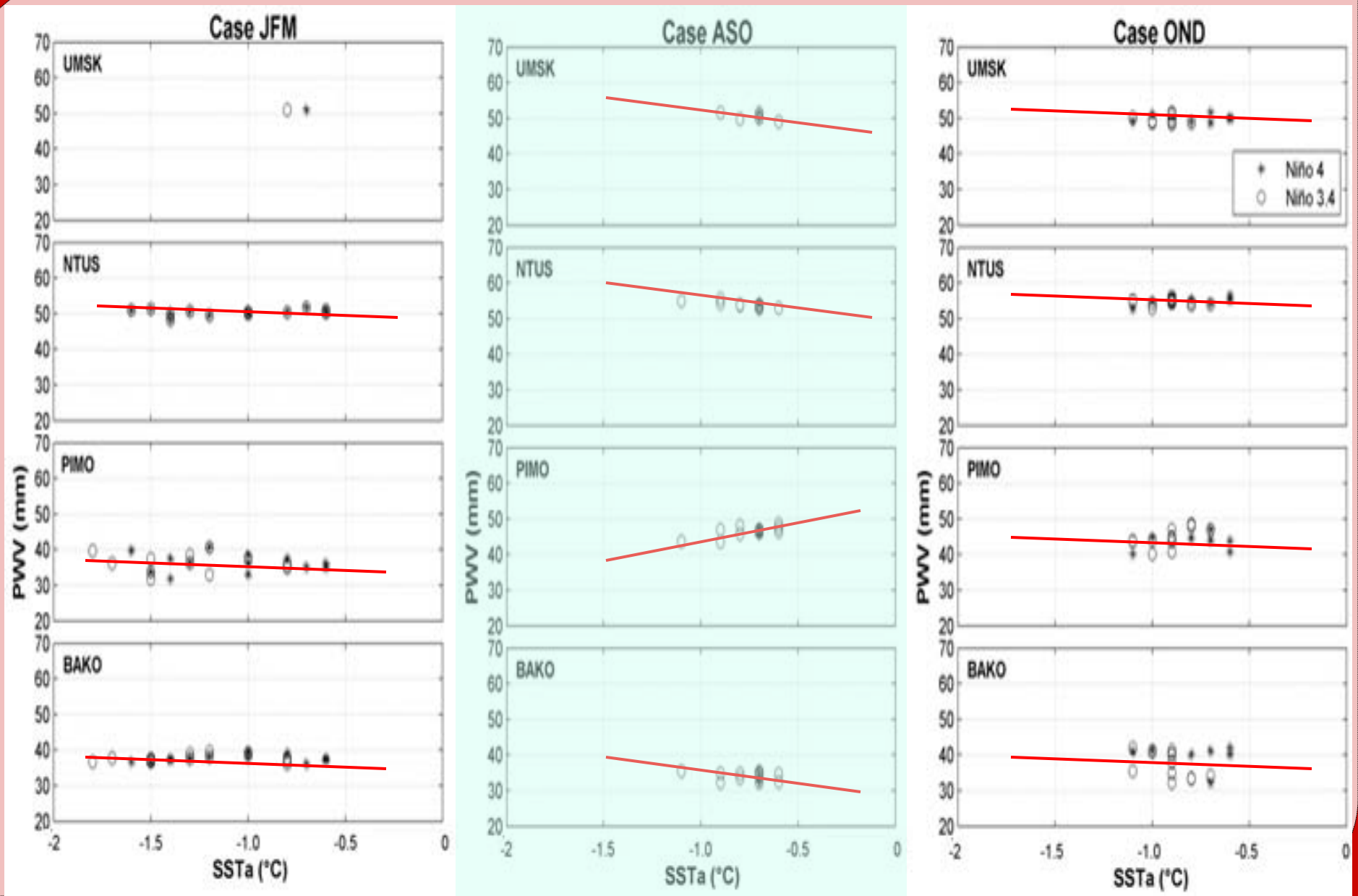

Acc. Rainfall every 3 month

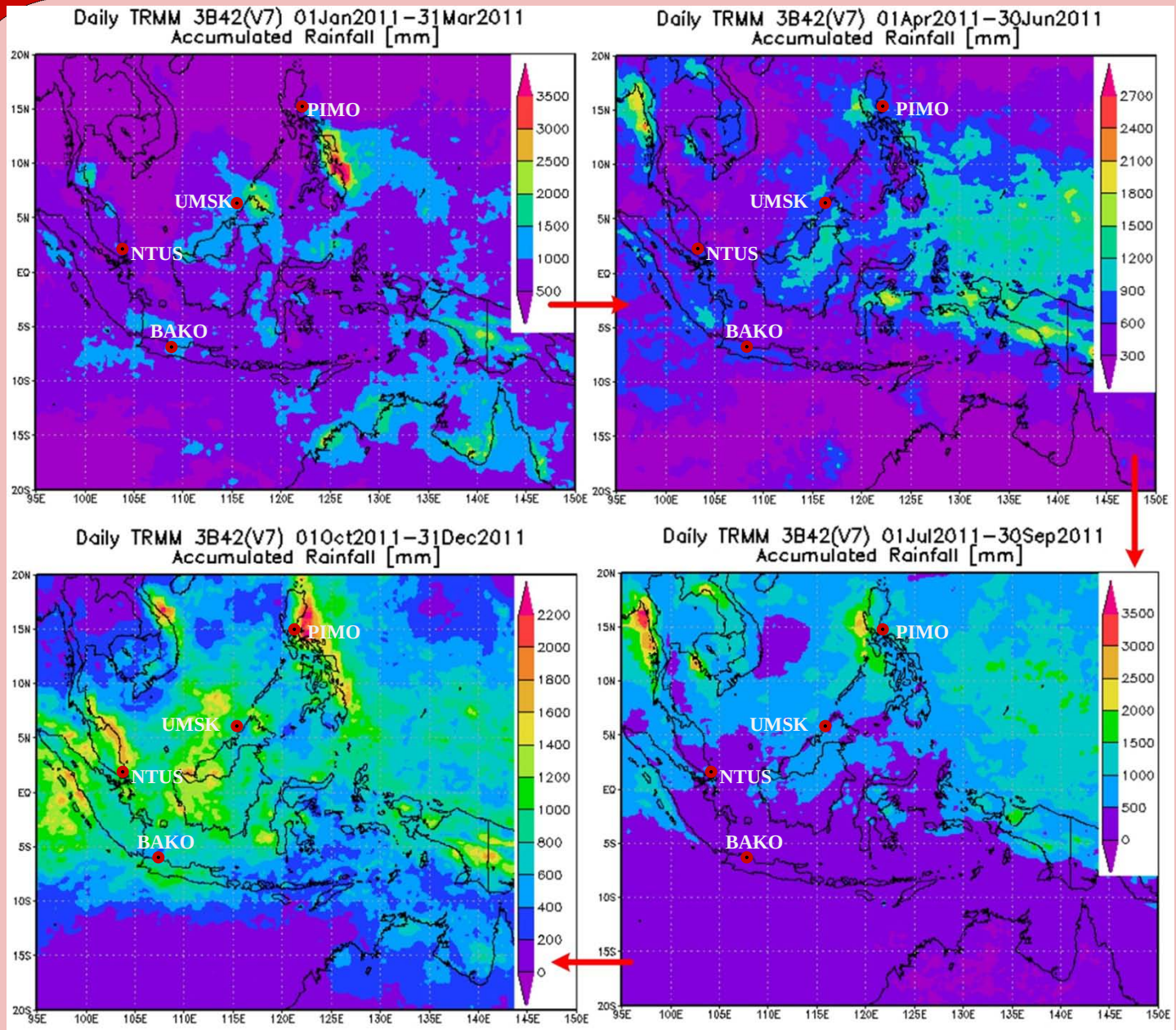

Higher rainfall was occurred in Philippines for JAN & DEC impact to PIMO and TANAY.

- Low rainfall during AMJ
- Moderate rainfall for JAS

El Nino case

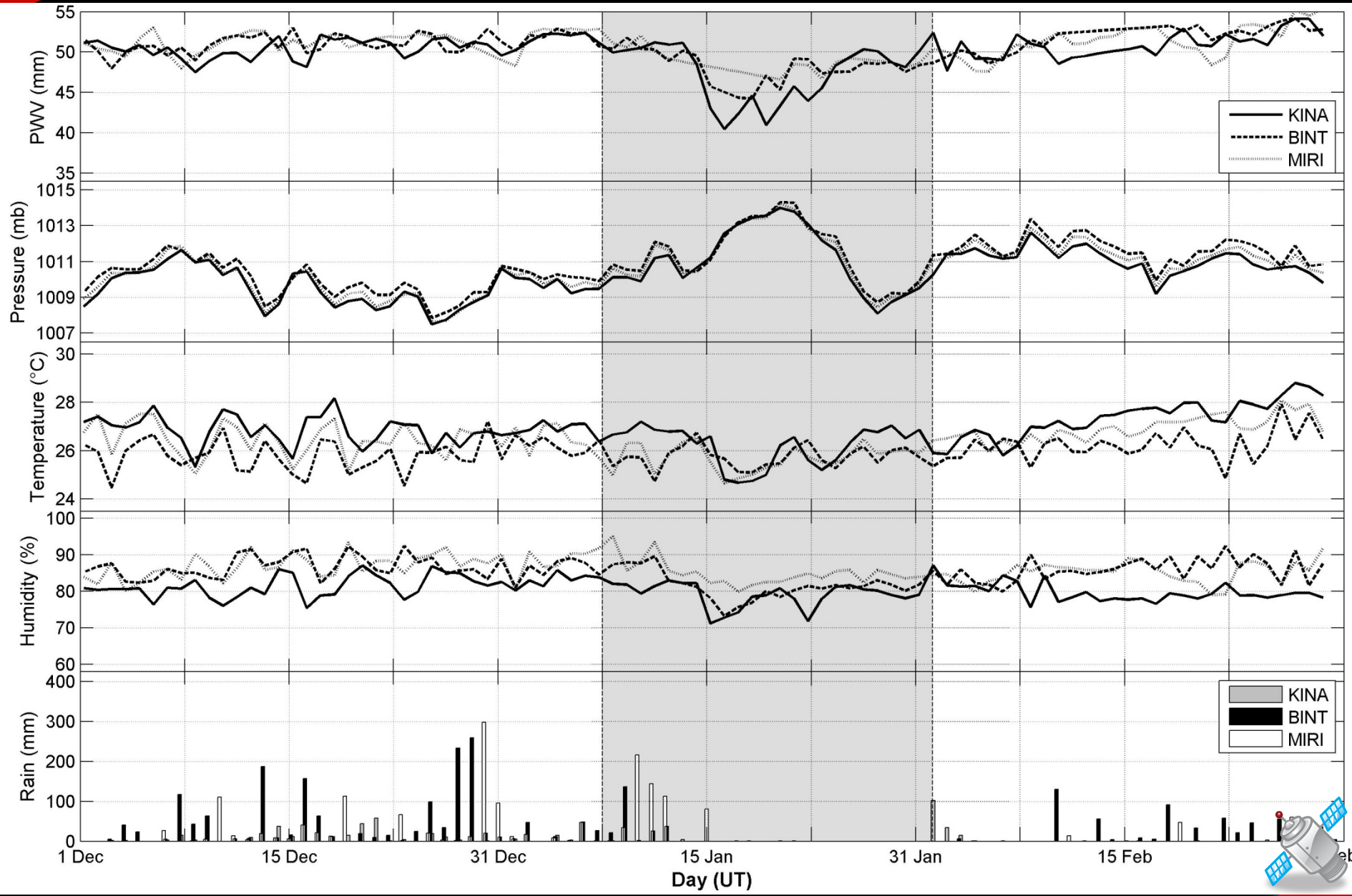
PWV (mm)
55
50
45
40
35
KINA
BINT
MIRI
Pressure (mb)
1015
1013
1011
1009
1007
Temperature (°C)
30
28
26
24
Humidity (%)
100
90
80
70
60
Rain (mm)
400
300
200
100
0
KINA
BINT
MIRI
1 Dec
15 Dec
31 Dec
15 Jan
31 Jan
15 Feb
Day (UT)

How ENSO affect the GPS signal?

- La Niña event associated with unusually wet conditions and correlated well with rainfall. More La Niña event occurred will be more decreasing in water vapor in the atmosphere because of condensation.
- Conversely for El Niño, it is characterized by unusually warm ocean temperatures in the Equatorial Pacific.

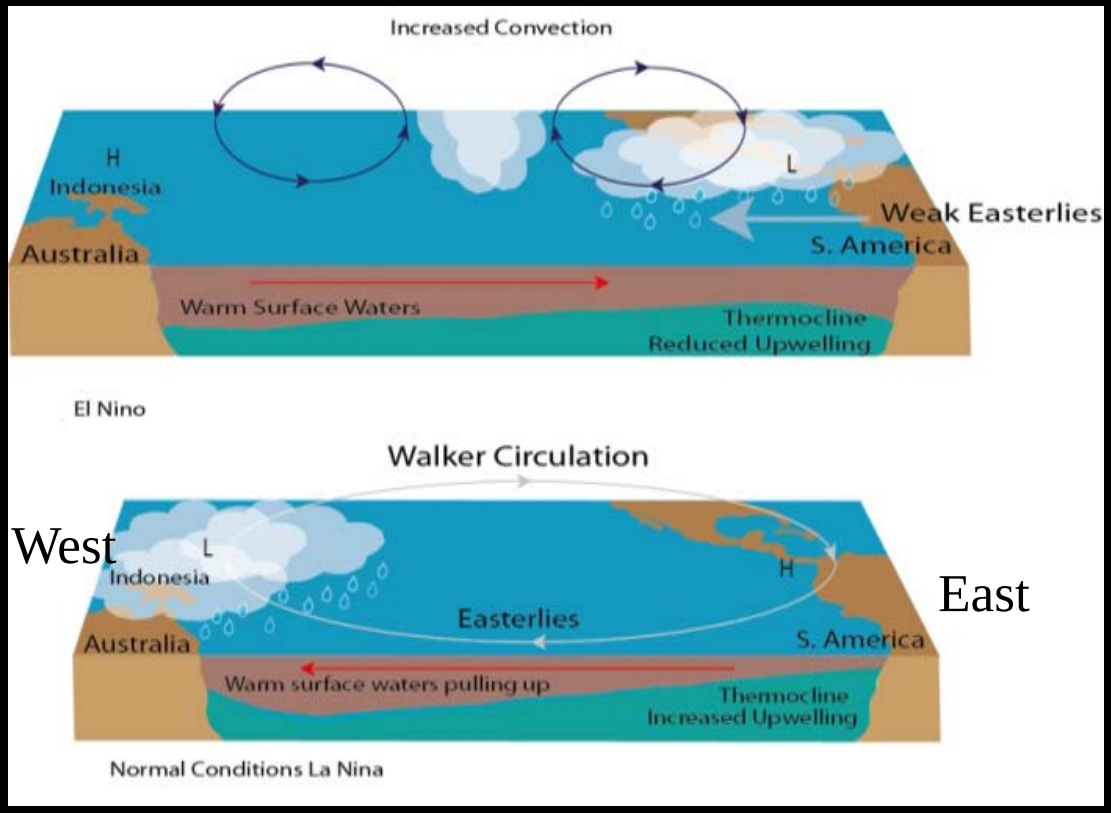

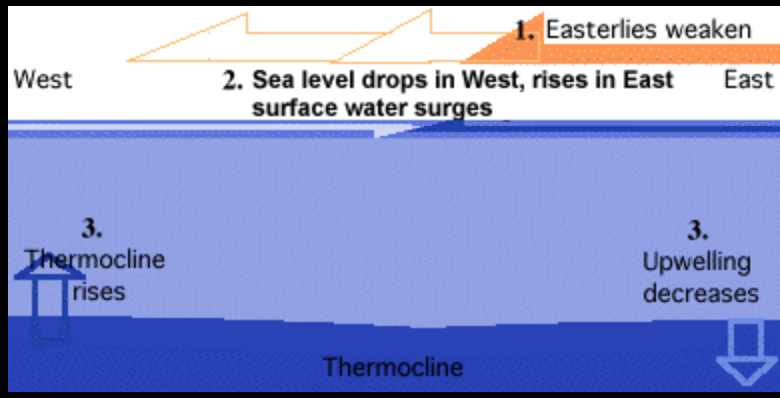

El Niño: *Because of more convection, low moisture occurs in the atmosphere and the surface ocean will be warm and decreased the latent heat of sea surface temperature (SST).*

EX2: PWV estimation using ANFIS

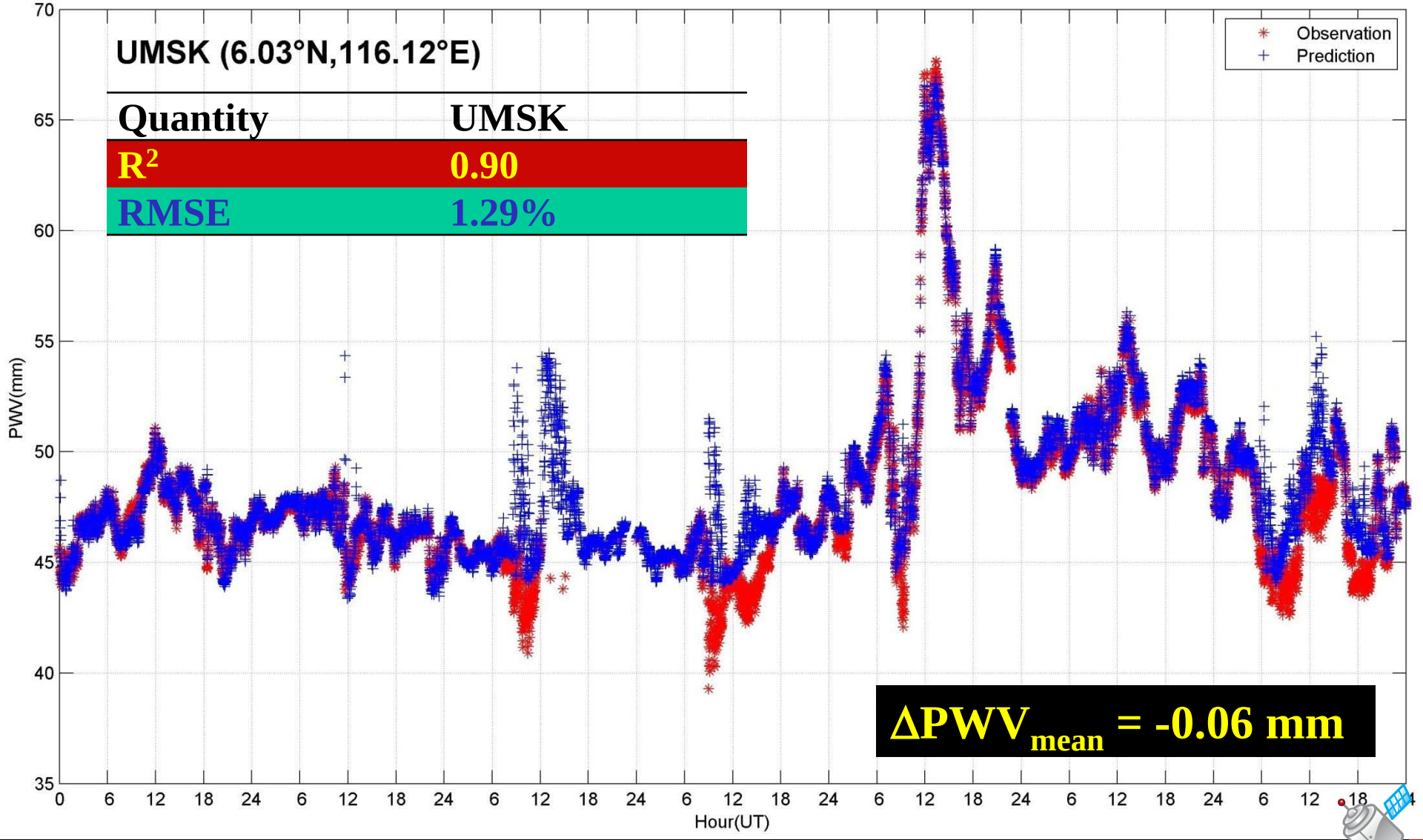

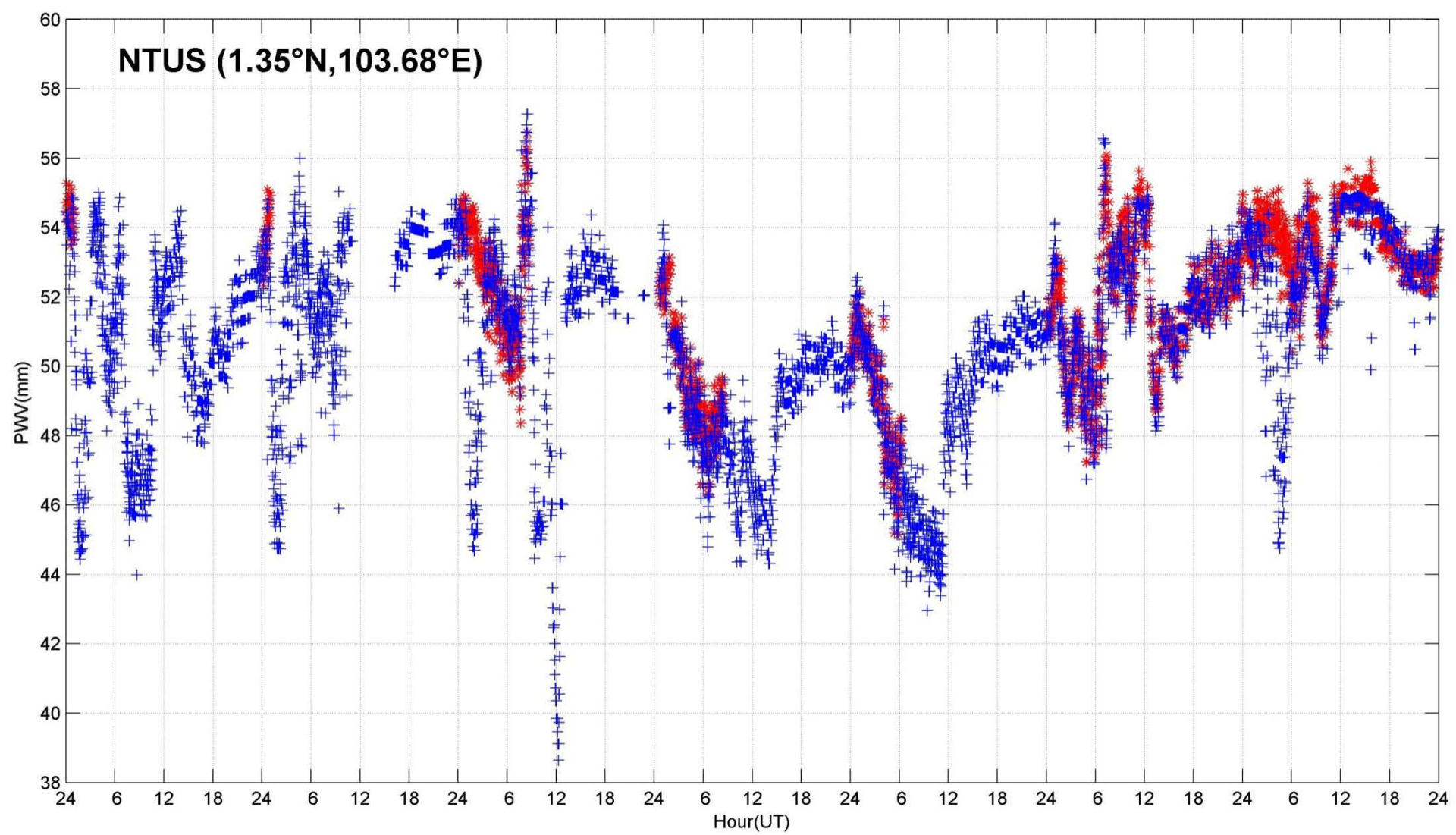

Quantity	UMSK
R^2	0.63
RMSE	1.68%

ΔPWV_{mean} = -1.31 mm

ANFIS Algorithm

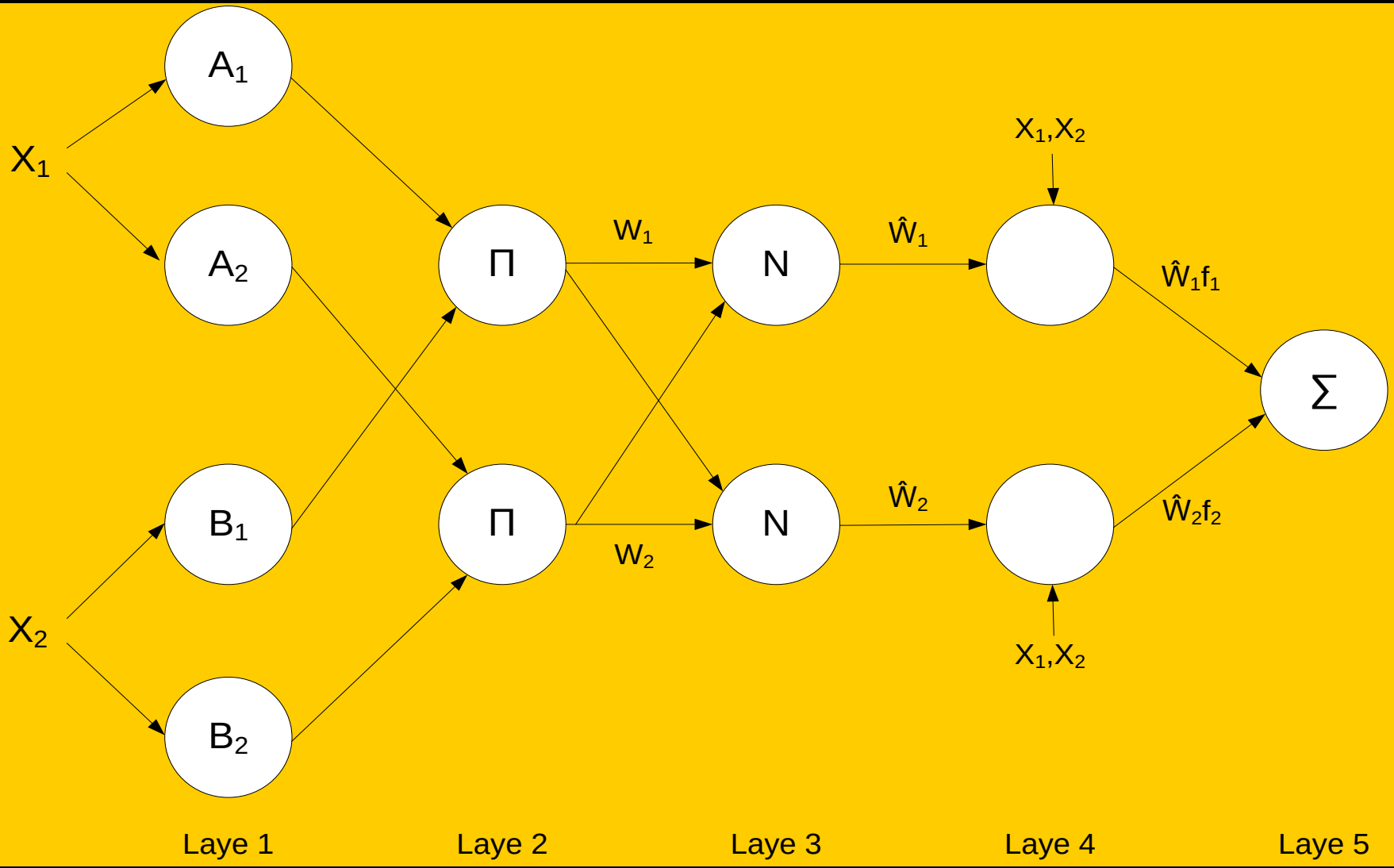

Input

AND operator

Normalized firing strengths

Consequent parameters

Adaptive neuro-fuzzy inference system (ANFIS)

The reasoning mechanisms on this Sugeno model after training by ANFIS is obtained as,

$$f_1 = 0.1309P + 2.567T + 0.6413H \pm 196.9$$

$$f_2 = 0.06896P + 2.991T + 0.6319H \pm 157.3$$

$$f_3 = -0.1251P + 2.851T + 0.6539H + 39.91$$

$$f_4 = 0.3626P + 3.031T + 0.8667H \pm 421.5$$

The PWV model using ANFIS:

$$\mathrm{PWV} = \frac{W_1 f_1 + W_2 f_2 + W_3 f_3 + W_4 f_4}{W_1 + W_2 + W_3 + W_4} = \overline{W_1} f_1 + \overline{W_2} f_2 + \overline{W_3} f_3 + \overline{W_4} f_4$$

Some Notes (Summary)

Scientific achievement of SCAR (Scientific Committee on Antarctic Research) agenda in 2011:

- Because of the lack in GNSS high-rate sampling receiver coverage over polar regions, particularly in Antarctica, the Action Group will contribute to answering questions that are still open within the Sun-Earth interactions studies. Some of the current issues in scientific international debate of particular interest are:
  - characterization of the cause-effect mechanisms driving the formation and evolution of ionospheric irregularities;
  - distribution and evolution of precipitable water vapor in polar regions which play a key role in the characterization and evolution of global earth phenomena.

Proposed observations

North Pole

EQ

South Pole

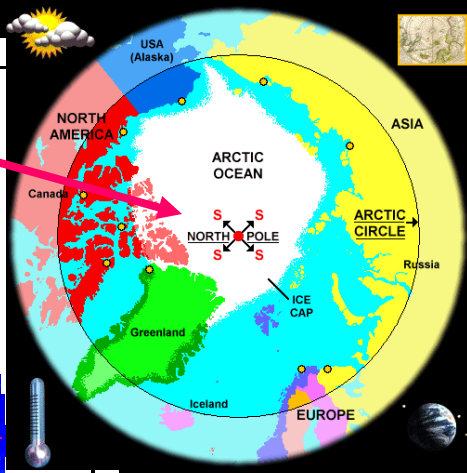

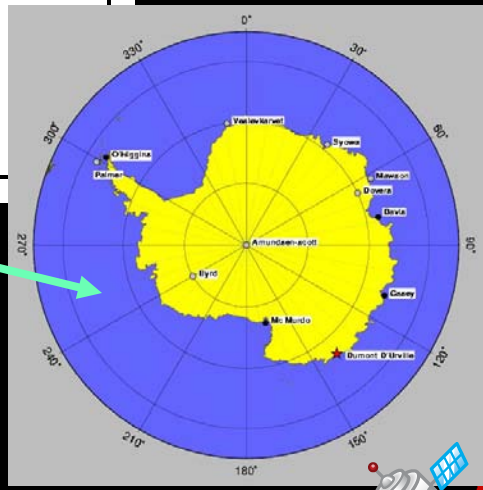

Teleconnections

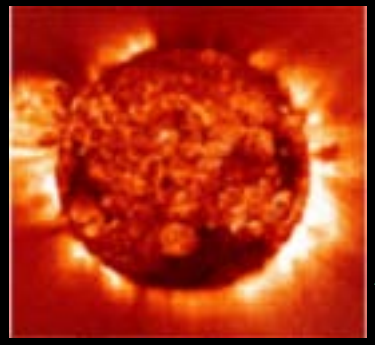

Solar

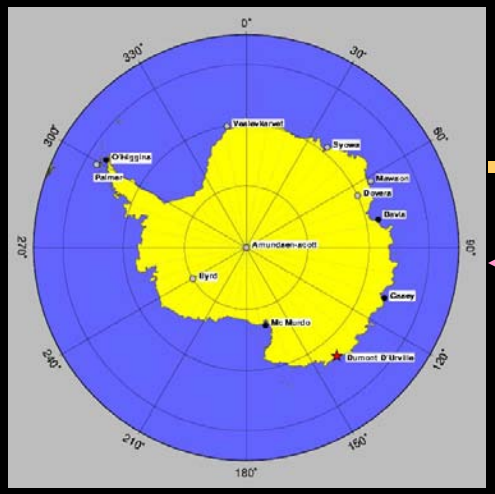

Terrestrial

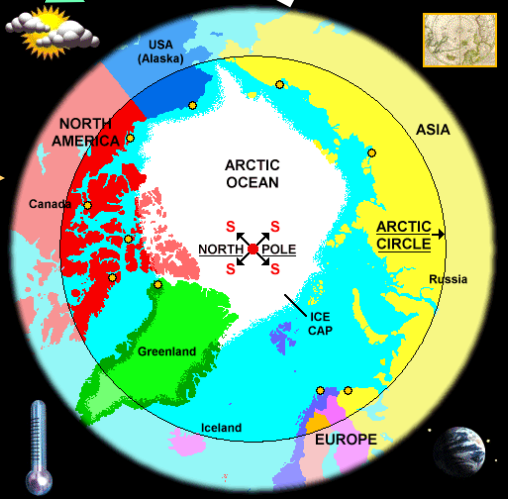

Teleconnections

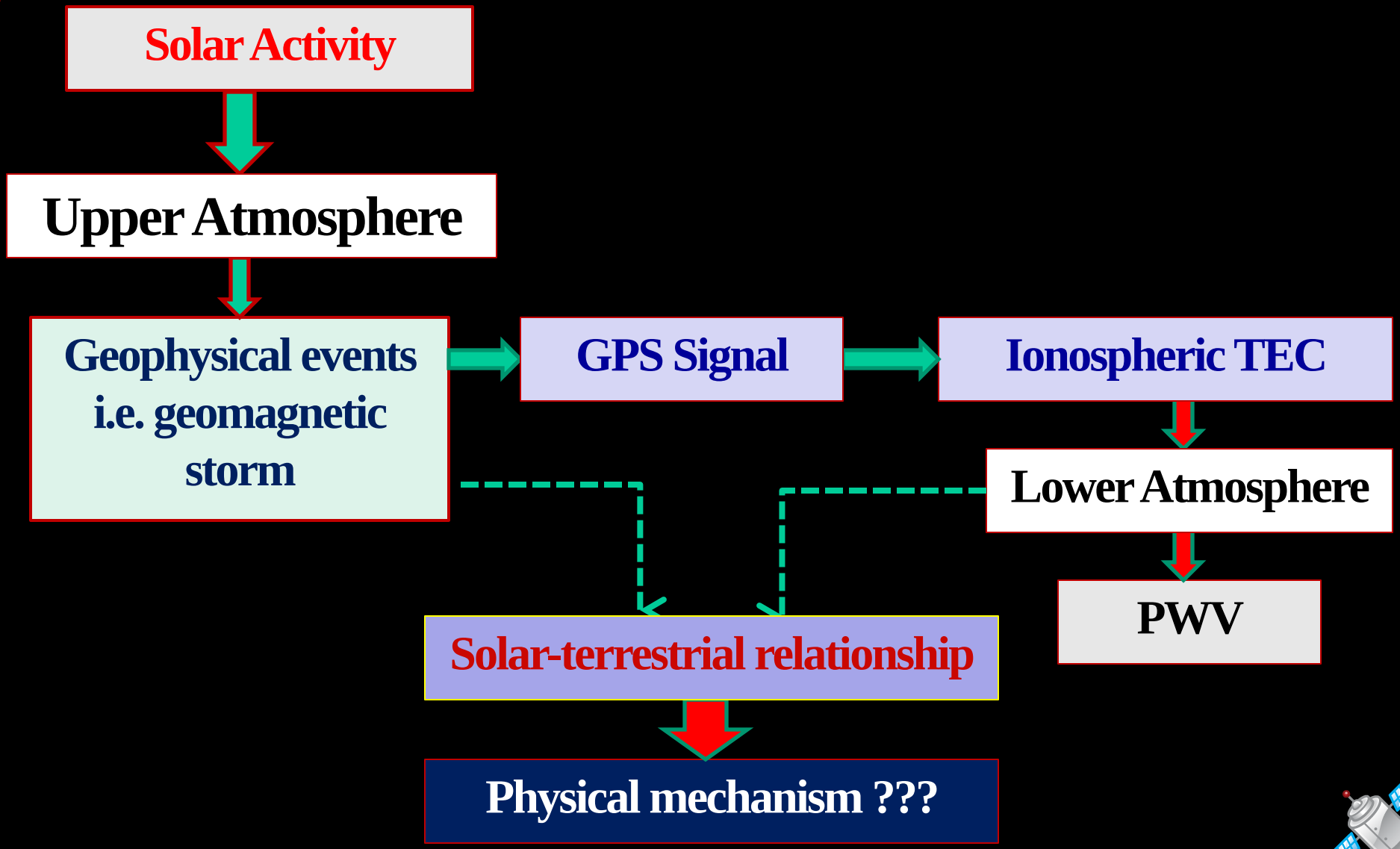

Ionospheric-tropospheric coupling

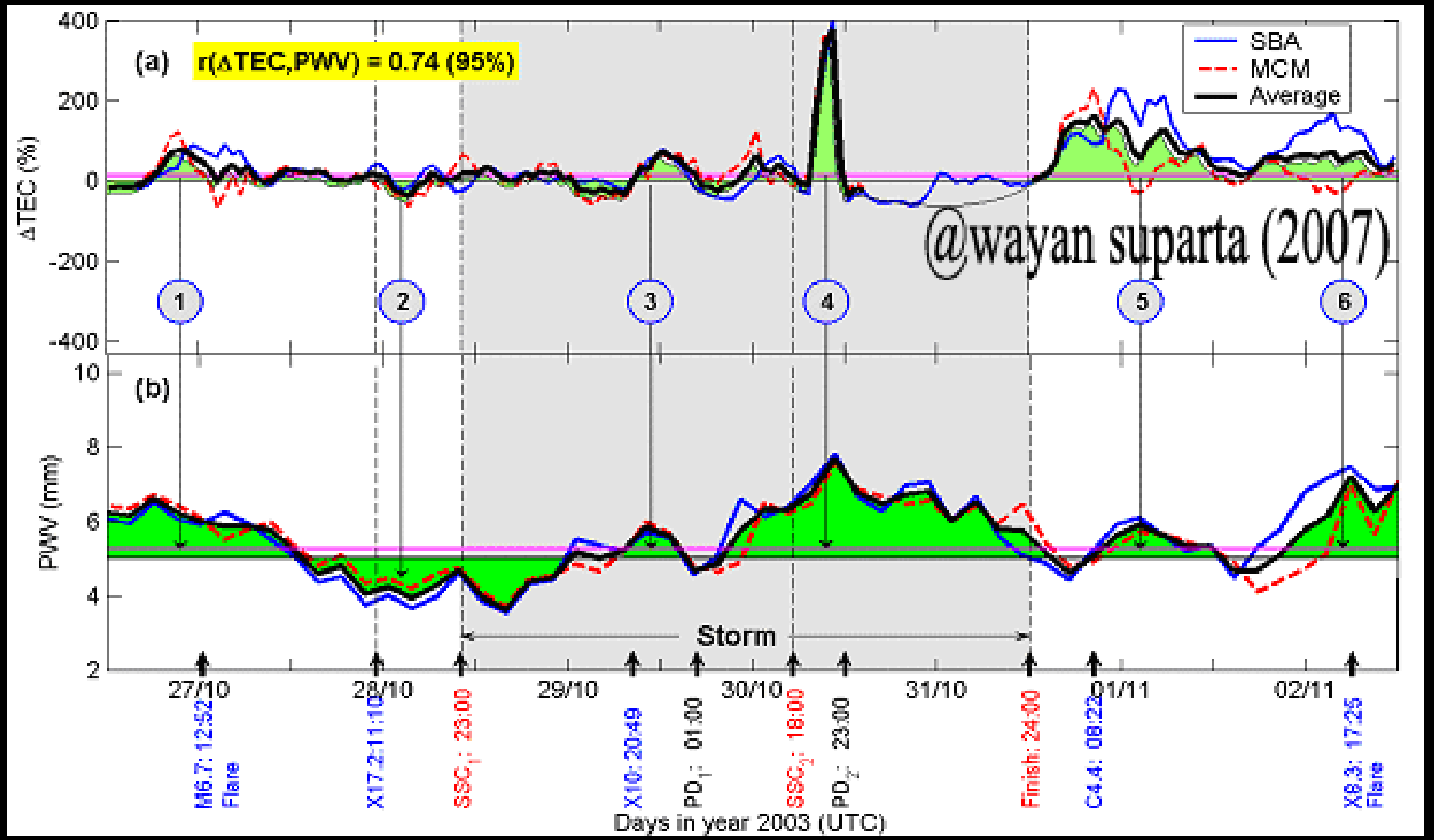

During Halloween storms of 2003 (Suparta et al., 2008: JASTP)

Global electric circuit identification

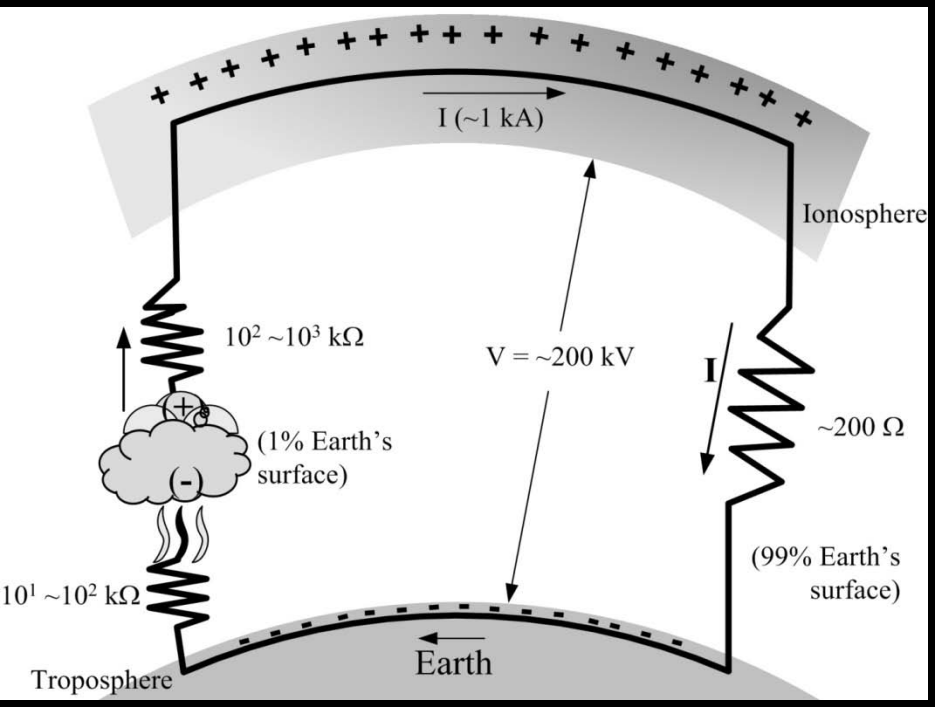

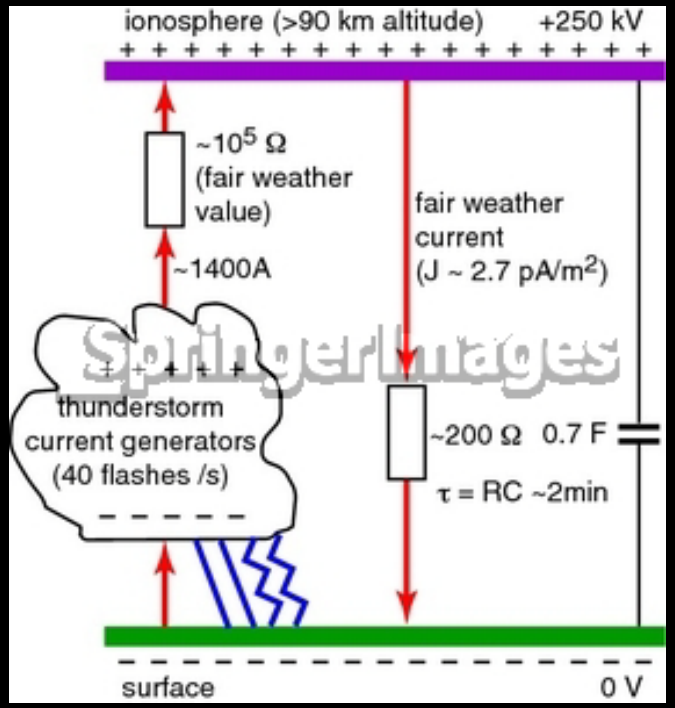

- The increase in TEC indicates substantial disturbances to the global atmospheric circuit (GEC), through an increase in the incident density of energetic particles in the atmosphere, and a major change in the conductivity in and above the ionospheric D-region.
- The above thundercloud positive charge seen is transferred to the conducting upper atmosphere, while the negative charge is transferred to the Earth. These GEC complex variations will depends on geographic position, magnetospheric and ionospheric processes, and also climate change.

Connecting Ionosphere-Troposphere

Roble and Tzur (1986)

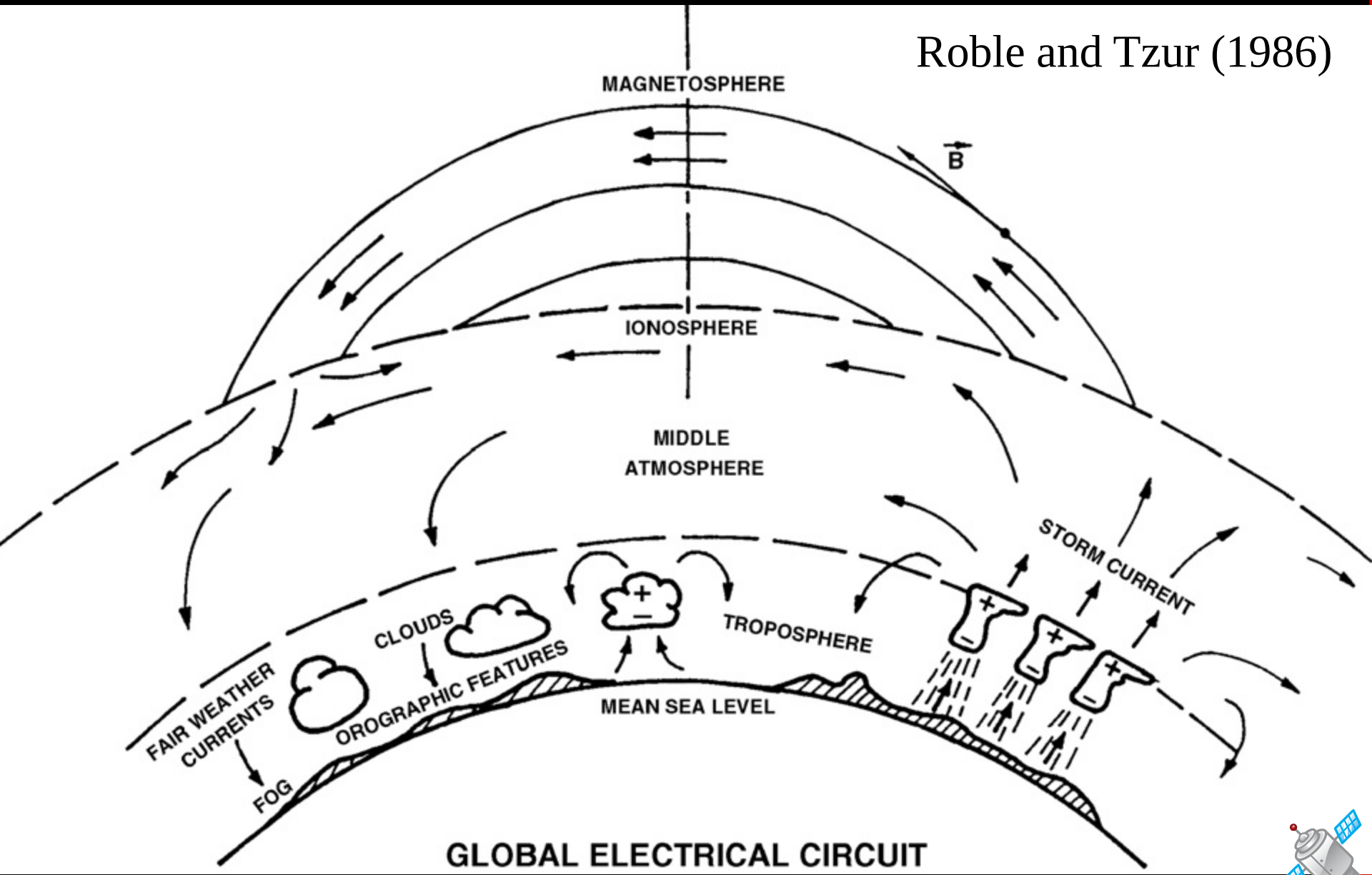

GEC proposed models

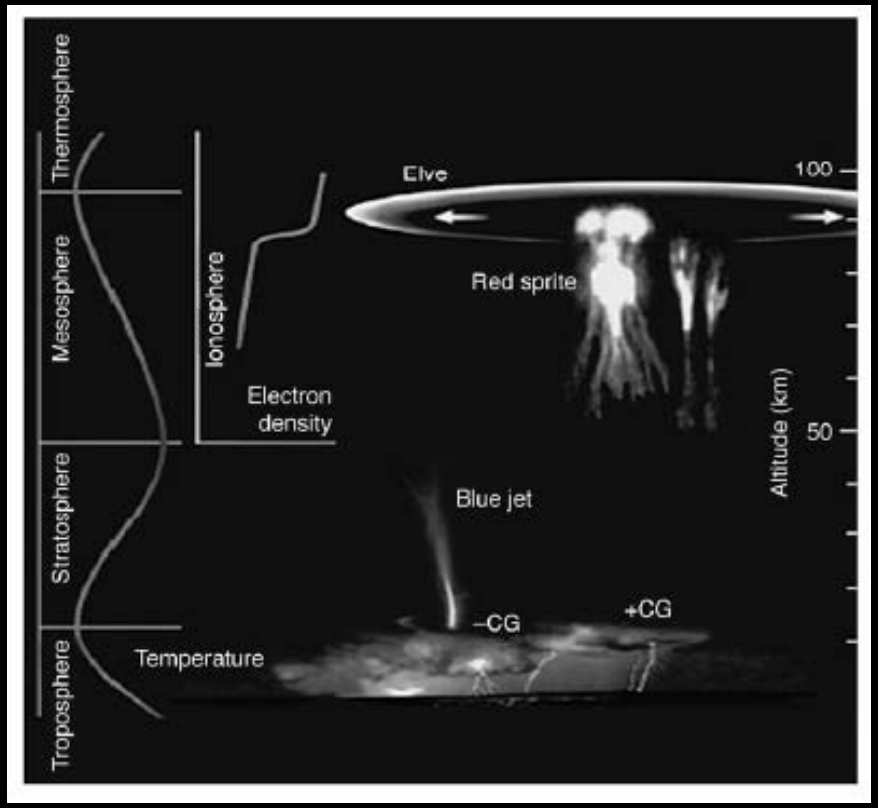

Tinsley (2000), Dsiingh et al. (2007)

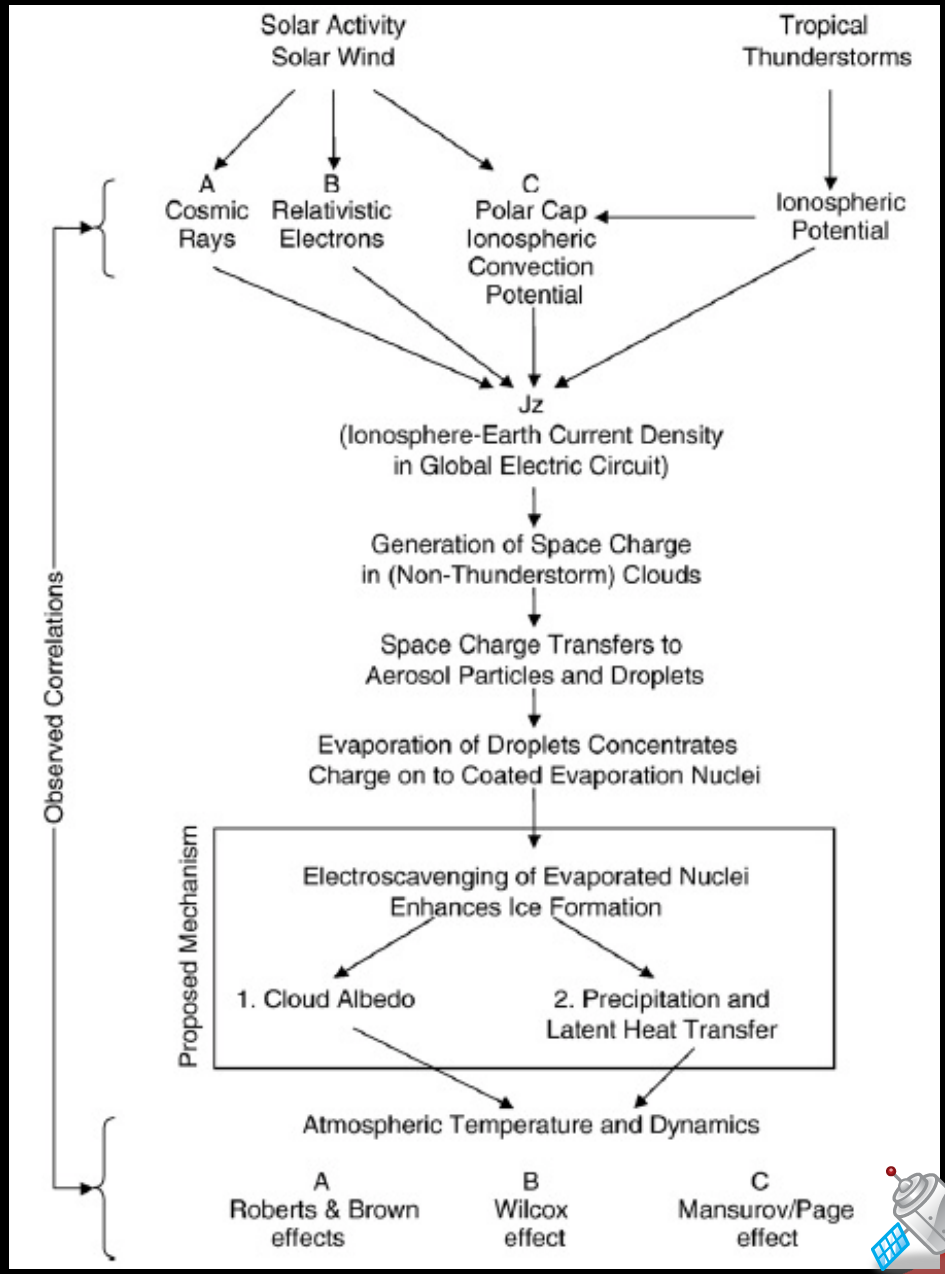

The beneficial of GPS

GPS sources:

- AKDA GPS Network
- BARD GPS Network
- BARGN GPS Network
- CORS GPS Network
- CRTN GPS Network
- CVSRN GPS Network
- EBRY GPS Network
- FSL GPS Network
- GAMA GPS Network
- GEONET GPS Network
- IGS GPS Network
- PANGA GPS Network
- PBO GPS Network
- PGF GPS Network
- SCIGN GPS Network
- SNG GPS Network
- UNAM GPS Network
- UNKNOWN GPS Network
- WCDA GPS Network

- http://sopac.ucsd.edu/dataArchive/ [GPS and Met data]
- CDDISA: ftp://cddisa.gsfc.nasa.gov/gps/products/ionex/
- AIUB: ftp://ftp.unibe.ch/aiub/CODE/ (DCB data)

Global Electron Content (GEC)

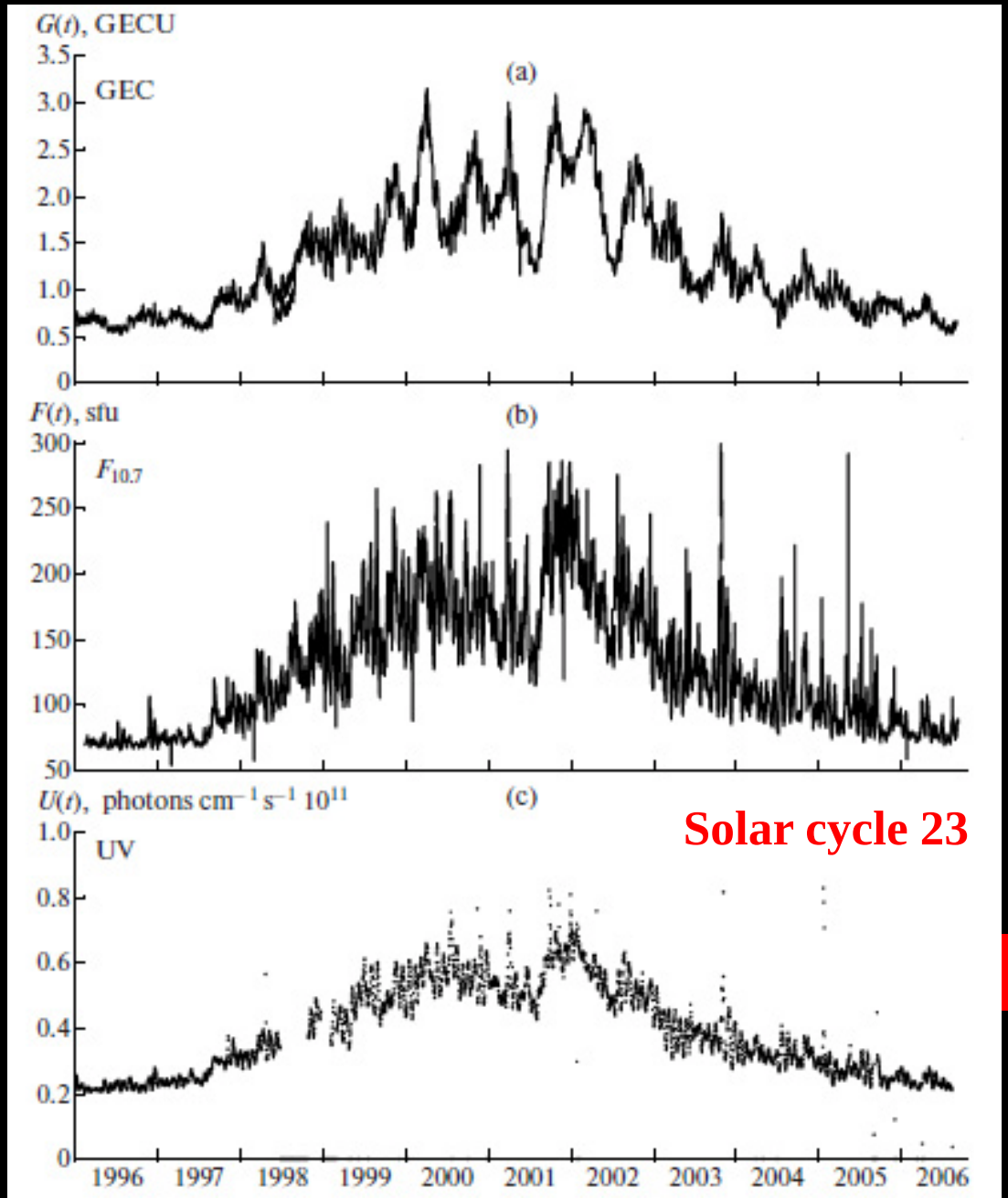

Solar cycle 23

- GEC is a new parameter was first proposed by Afraimovich et al. (IRI News, 2006)
- GEC is equal to the total number of electrons in the near-Earth space.
- GEC (in GECU) is better than local TEC that reflect the global response to a change of solar activity.

Antarctic Stamp Launching

The National Science Centre, Bukit Kiara on 8 March 2012

Commemorative Stamps and First Day Cover of the Malaysian Antarctic Research Programme (MARP) was launched by Datuk Seri Panglima Dr. Maximus Johnity Ongkili, Minister of Science, Technology and Innovation (MOSTI)

Memory of Antarctic Research

Utusan Malaysia, 6 March 2012

Thank you. Terima kasih!

Q/A